

Atomic-level Heterogeneity and Defect Dynamics in Concentrated Solid-Solution Alloys

Yanwen Zhang^{a,b}, Shijun Zhao^a, and William J. Weber^{b,a}

^a *Materials Science and Technology Division, Oak Ridge National Laboratory, Oak Ridge, TN 37831, USA*

^b *Department of Materials Science and Engineering, The University of Tennessee, Knoxville, TN 37996, USA*

Kai Nordlund^c, Fredric Granberg^c, and Flyura Djurabekova^{c,d}

^c *Department of Physics, P. O. Box 43, FIN-00014 University of Helsinki, Finland*

^d *Helsinki Institute of Physics, P. O. Box 43, FIN-00014 University of Helsinki, Finland and*

ABSTRACT

Performance enhancement of structural materials in extreme radiation environments has been actively investigated for many decades. Traditional alloys, such as steel, brass and aluminum alloys, normally contain one or two principal element(s) with a low concentration of other elementals. While these exist in either a mixture of metallic phases (multiple phases) or solid solution (single phase), limited or localized chemical disorder is a common characteristic of the main matrix. In sharp contrast to the traditional alloys, recently developed single-phase concentrated solid solution alloys (CSAs) contain multiple elemental species in equiatomic or high concentrations with different elements randomly arranged on a crystalline lattice. Due to the lack of elemental predictability in these CSAs, they exhibit significant chemical disorders and unique site-to-site lattice distortions. While it has long been recognized that specific compositions of traditional alloys have enhanced radiation resistance, it remains unclear how the atomic-level heterogeneity affects defect formation, damage accumulation, and microstructural evolution. Such knowledge gaps have been a roadblock to future-generation energy technology. CSAs with a simple crystal structure, but complex chemical disorder are ideal systems to understand how compositional complexity influences defect dynamics, and to fill the knowledge gaps with focus on electronic- and atomic-level interactions, mass and energy transfer processes, and radiation resistance performance. Recent advances of defect dynamics and irradiation performance of CSAs are reviewed, intrinsic chemical effects on radiation performance are discussed, and future directions are suggested.

Key words: chemical disorder; concentrated solid-solution alloys; lattice distortion; energy landscapes; defect dynamics; microstructure evolution; irradiation effects

Corresponding author: zhangy1@ornl.gov (Y. Zhang Oak Ridge National Laboratory, Ph: 865-574-8518, Fax: 865-241-3650), wjweber@utk.edu (William J. Weber), kai.nordlund@helsinki.fi (K. Nordlund), and flyura.djurabekova@helsinki.fi (F. Djurabekova)

This manuscript has been authored by UT–Battelle, LLC under Contract No. DE–AC05–00OR22725 with the U.S. Department of Energy. The United States Government retains and the publisher, by accepting the article for publication, acknowledges that the United States Government retains a non-exclusive, paid-up, irrevocable, world-wide license to publish or reproduce the published form of this manuscript, or allow others to do so, for United States Government purposes. The Department of Energy will provide public access to these results of federally sponsored research in accordance with the DOE Public Access Plan.

1. Introduction

Ever since ancient civilization, development and improvement of metallic alloys with better structural strength or improved functionalities have repeatedly changed the world and enriched the breakthroughs that are provided to meet human needs. Useful alloys have typically comprised multiple phases, with one or two dominant elements modified by small additions of other elements. Conventional approaches typically take a material that empirically has good properties, and make small changes in composition and microstructure to achieve more desired performance, such as improved radiation tolerance. For discussion purposes in this work, most of these alloys being studied in the past or used in various applications are termed as *traditional alloys*. Such traditional alloys are also commonly referred as dilute alloys, with the major element as a solvent and alloying elements as a solute.

In sharp contrast to traditional alloys, concentrated solid solution alloys (CSAs), consisting of two to five (or more) elemental species all at high concentration, have recently attracted increasing attention and intensive research effort [1-3]. The newly developed multi-component systems with five or more elements, typically near equiatomic composition, are commonly termed high entropy alloys (HEAs), wherein the configurational entropy is higher than the entropy of melting of most common metals [4-6]. Instead of ordered intermetallics from classical physical metallurgy, a direct consequence of thermodynamic stabilization of some high-entropy phases is a reduction of the thermodynamic driving force towards oxidation and phase transformation. Both face centered cubic (fcc) and body-centered cubic (bcc) CSAs, including HEAs, with a strong tendency to solid solution strengthening have been produced. These *non-traditional alloys* exhibit strong resistance to softening (high strength and low plasticity) at high temperatures, and excellent tensile strength at low temperatures, which makes them candidate materials for many potential applications, including high-temperature thermal stability and hardness [7-9], improved fatigue, strength, ductility, and fracture resistance [3,10,11], improved irradiation resistance [2,12-14] and excellent corrosion and wear resistance [5].

Intense radiation in nuclear fission and fusion power systems transfers energy to electrons and atoms in the material, and produces defects. Structural materials in advanced nuclear reactor components, such as iron-based alloys (the primary basis for structural materials), must demonstrate long-term stability and tolerance to radiation damage at elevated temperatures over long lifetimes. It is known that the accumulation of defects may ultimately compromise the material's strength and performance lifetime. Historically, alloy development in traditional alloys with improved radiation performance has been focused on addition of alloying elements or nanoscale features with complex microstructures to mitigate damage. To move beyond the current knowledge and incremental radiation resistance property improvements in traditional alloys, we must understand the roles of all constituents in alloys and their atomic-level heterogeneity effects on defect evolution in a radiation environment.

The current opinion and developments in this article will focus on single-phase CSAs with HEAs as part of the family. The constituent elements in these CSAs are distributed randomly on a crystal lattice, such as fcc, bcc, or hexagonal close-packed (hcp). While retaining a simple macroscopically crystalline structure, such random occupancy of different elemental species (extreme *chemical complexity*) creates unique site-to-site lattice distortions and locally disordered chemical environments, leading to extreme intrinsic complexity at the electronic and atomic levels [2,12,15,16]. In extreme cases such as in HEAs, no element will have the same nearest and second nearest neighbor environment [2,15]. Such unusual lattice distortions have demonstrated significantly improved radiation resistance attributing to the high atomic-level stresses facilitating rapid recrystallization and preventing extended dislocation formation.

Recent research has focused on how alloy complexity in single-phase CSAs affects defect dynamics and microstructure evolution by varying the number, type and concentration of alloying elements [2,12-14,17]. This article reviews compositional effects on radiation performance in traditional alloys and informs on current progress of radiation effects in CSAs, including unique energy landscape of CSAs and atomic-level understanding on defect dynamics at both short- and long-time scales. Challenges and future directions are discussed. In this special issue, the *Physical Metallurgy of Concentrated Solid Solutions from Low-Entropy to High-Entropy Alloys* is reviewed by Yeh *et al.*, the *Phase Stability,*

1 *Physical Properties and Strengthening Mechanisms* by Bei *et al.*, the *Thermodynamics of Concentrated*
2 *Solid Solution Alloys* by Gao *et al.*, the *Mechanical properties of solid solution high- and medium-entropy*
3 *alloys* by George *et al.*, and the *Fundamental Deformation Science in Multiphase High Entropy Alloys* by
4 Liaw *et al.*

5 **2. Traditional alloys: compositional effects on radiation performance**

6 Alloying elements at low-concentrations into pure metals is the traditional approach in the long
7 history of alloy development, and is widely used to achieve desired materials properties, such as better
8 yield strengths and enhanced radiation tolerance. In many dilute solid solutions, numerous experimental
9 observations, with some specific examples reviewed below, have shown that substitutional additions at a
10 certain amount can significantly improve or degrade radiation performance. While many possible
11 explanations are proposed, no unified underlying mechanisms and validation are currently available.

12 A study of the Ni-Cu system displays a remarkable resistance to void formation under irradiation
13 [18,19]. In pure nickel samples, voids formed throughout the entire damage range under Ni irradiation,
14 but only appeared at the near-surface region and at the peak damage depth under Cu irradiation. The
15 effect of alloy additions on radiation response was performed later by the same group [20] in pure nickel
16 and two Ni-Cu alloys with pre-implanted He. The results show that the density of both dislocation loops
17 and helium bubbles increases with increasing copper content, while the size decreases. The authors
18 speculated that nanoscale Cu particles might exist in the Ni-Cu alloys to disperse vacancies and gas
19 atoms, thereby suppressing the swelling. This statement was not confirmed due to the limited detection
20 resolution of transmission electron microscopy (TEM) available at that time. With today's knowledge,
21 one question to ask is whether such a significant difference in radiation behavior results from the nano-
22 scale precipitates, from alloying effects (interplays between Ni and Cu) in the solid solution form, or from
23 the combination of the two.

24 In the Ni-Al binary alloy system with Al levels ranging from 1.1 to 13.3 wt%, irradiation
25 responses were investigated at temperatures ranging from 400 to 650 °C in the EBR-II fast reactor [21].
26 The irradiation-induced density changes were found to strongly depend on both Al content and irradiation
27 temperature. The results clearly show that the progressive addition of Al decreases the swelling to ward a
28 saturation level at lower irradiation temperatures. At higher temperatures, there is a tendency for swelling
29 to increase again at the higher Al levels. Although the importance of Al content is clearly observed, the
30 underlying mechanisms to explain these observations are missing. In this study, the Al concentration
31 varied from a few percent in a dilute alloy to a more concentrated solid solution alloy with an Al
32 concentration over ten percent. Defect and mass transport in dilute alloys have been studied intensively,
33 the transport property in concentrated solid-solution alloys is, however, much less understood [14,22,23].
34 A key challenge for the Ni-Al work is to understand alloying effect on migration barriers and paths for
35 both interstitials and vacancies as a function of Al concentration and temperature, especially near the
36 percolation threshold of mass transport.

37 Physical, chemical and mechanical properties of metallic solid solutions are often thought to be
38 affected by a difference in atomic size between the solvent and solute elements [24] in traditional alloys.
39 The effects of volume size factor of solute atoms (a measure of the dilation caused by a solute) have been
40 studied [25] in He-irradiated Ni-based alloys at 500°C. The swelling results of pure Ni, Ni-Si, Ni-Co, Ni-
41 Cu, Ni-Mn and Ni-Pd alloys show that volume size factors strongly affect the radiation-induced swelling.
42 The number density of bubbles as well as the mean size increased with the volume size factor. Such
43 observations imply that both the irradiation-induced point defects and the mobility of helium are
44 influenced by elemental species and chemical disorder, which calls attention to elemental effects or
45 chemical effects on defect dynamics.

46 Strong compositional dependence to irradiation response is also observed in the V-Fe binary and
47 V-Fe-Ti ternary systems [26]. A systematic increase in cavity size was observed with increasing Fe
48 concentration. The void swelling of pure V is low after irradiation to ~11 displacements per atom (dpa) at
49 a range of temperatures. Alloying low concentration of Fe (5%) leads to a dramatic increases in swelling,

1 up to 30%. Addition of low levels of Ti to the V-5Fe alloy leads to suppression of swelling. In each case,
2 the authors report that the solutes remain in the solution. A similar result has been reported more recently
3 for various Ti contents in V-Ti alloys and Fe contents in V-Fe alloys under He irradiation [27]. Increase
4 of Ti concentration in V-Ti alloys leads to reduced swelling, which is attributed by the authors to local
5 regions of compression resulting from the oversized Ti atom in V lattice. On the other hand, when
6 undersized Fe atoms replace V atoms, it is believed that sites for sinks of interstitial atoms are formed to
7 interact with He. The arguments based on the impact of under-sized and over-sized solutes for the
8 observed sensitivity clearly demonstrate the importance of atomic-level understanding of elemental
9 effects (localized tensile or compression stress resulting from the lattice distortion) to material
10 performance.

11 Commercial high-strength Ni-Cr systems were developed in the 1950-1960s for blades of jet
12 engine turbines. Properties of some Ni-Cr alloys have been studied, aiming to determine the possibility of
13 their use as structural materials for nuclear reactors [28-30]. While the absence of gas-vacancy pores in
14 these alloys indicated a low concentration of vacancies and low mobility of transmutation He, the low
15 dislocation density suggested a low concentration of interstitial atoms. The low defect concentration
16 (vacancies and interstitials) presented from these studies may, however, be viewed as an outcome of
17 tailoring chemical complexity to control defect evolution through suppressed defect production and
18 enhance recombination at an early stage – a path forward for designing special structural alloys with
19 improved radiation resistance [2,12].

20 There are many studies on the Fe-based alloys that have indicated significant impacts of
21 composition and chemistry on defect production and evolution. The Fe-Cr binary alloys are a base for low
22 activated ferritic-martensitic steels used widely as structural materials for fission reactors and currently
23 being considered as candidate materials for future fusion reactors. A series of studies of irradiation
24 behavior of Fe-Cr alloys and pure Fe has been undertaken in an attempt to elucidate the basic mechanisms
25 of defect formation, void swelling and low temperature irradiation-induced embrittlement in ferritic-
26 martensitic steels [31-36]. Microstructural changes induced from radiation damage in Fe and Fe-Cr alloys
27 have also been investigated as a function of irradiation temperature, ion/neutron fluence, and Cr content
28 under triple-beam irradiation (D^{2+} , He^+ , Fe^+) [37]. The composition dependence of swelling on Cr
29 concentration is explained in terms of different binding interactions between Cr solute atoms and
30 irradiation-produced vacancies, as well as the difference in sink strength of microstructural features. More
31 recently, the evolution of radiation damage in Fe and Fe-Cr alloys under heavy-ion irradiation has been
32 investigated [38,39]. Dynamic observations are carried out under an electron microscopy where the
33 evolution of damage and the early stages in damage development show that, although small (2-4 nm)
34 dislocation loops first appeared at doses between 10^{12} and 10^{13} ions cm^{-2} in all samples, the number of
35 loops retained depended strongly on the foil orientation in pure Fe, but not in Fe-Cr alloys, with different
36 Cr content. The *in-situ* observations show hopping of very mobile $\frac{1}{2}\langle 111 \rangle$ loops in pure Fe under ion and
37 electron beam irradiations, and that many $\frac{1}{2}\langle 111 \rangle$ loops easily glided to the foil surface. Hopping of
38 dislocation loops is particularly pronounced in ultra-pure Fe, but occurs much less frequently in Fe-Cr
39 alloys. Lower loop mobility in Fe-Cr alloys is observed and attributed to possible pinning effects by Cr
40 atoms. One may wonder that if such pinning effects are a key control of defect dynamics, which may be
41 the most effective way to achieve the maximum density of pinning sites per unit volume. Considering the
42 random arrangement of multiple elemental species in CSAs, such atomic-level alternation would meet the
43 requirement that each atom can be in fact viewed as a pinning site — the most effective way to create the
44 maximum density of pinning sites per unit volume [2].

45 Changing the number of constituent elements and various compositions in more complex alloys,
46 defect production and damage evolution shows new features. In fcc alloys, point defect processes in
47 neutron irradiated Ni, Fe-15Cr-16Ni and Ti-added modified SUS316SS are reported recently [40]. Void
48 growth is discussed on the basis of the interactions of vacancies and interstitials with defect clusters. The
49 growth behavior of interstitial-type dislocation loops (I-loops), stacking fault tetrahedra (SFT) and voids
50 is found to be quite different among these specimens. While I-loops are developed at lower temperatures
51 in Ni than in Fe-15Cr-16Ni and modified SUS316, more swelling occurs in Ni than in Fe-15Cr-16Ni, and

no voids are observed in modified SUS316. There is a significant difference in defect structures between Fe-15Cr-16Ni and modified SUS316 due to low weight concentration of alloying elements of Ti, Si, Mo, Mn and C. The growth of SFT detected in Fe-15Cr-16Ni and modified SUS316 is explained by a change in the dislocation bias of SFT resulting from the absorption of alloying elements. These studies on alloys with increased compositional complexity have indicated significant impacts of alloying effects at the elemental level on defect production and evolution.

As a brief summary of the literature review on radiation response in traditional dilute alloys and some concentrated alloys, compositional complexity has shown clear influence on defect dynamics and radiation responses. The lack of a unified fundamental description of the effects of the compositional complexity on defect processes and irradiation performance poses a significant roadblock to alloy development for applications in extreme radiation environments. All the above experimental observations are pointing to a more general base: *substitutional solid solutions with increasing chemical complexity in terms of local disordered chemical environments and unique site-to-site lattice distortions may have a profound effect on fundamental processes in determining defect production and damage evolution.*

3. Non-traditional alloys: unique single-phase concentrated solid-solution alloys

3A. Concentrated solid solution alloys with tunable chemical complexity

CSAs compose of multiple elemental species randomly arranged on a simple crystalline structure. In these CSAs, the chemical complexity can be achieved by controlling the number, type, and concentration of the constituent elements. The composition of such CSAs can be at or near equiatomic or at concentration with one or two elemental species in large variation within the solubility limits, as noted in **Fig. 1**. These CSAs with different elements coupled inimitably show distinct properties at the level of electrons and atoms and allow a systematic study of defect dynamics and irradiation performance with increasing complexity.

While CSAs encompass HEAs, they can also be considered as subsystems of HEAs, such as subsets of $\text{Ni}_{25}\text{Cr}_{25}\text{Fe}_{25}\text{Co}_{25}\text{Pd}_{25}$ (NiCrFeCoPd) or $\text{Ni}_{25}\text{Cr}_{25}\text{Mn}_{25}\text{Fe}_{25}\text{Co}_{25}$ (NiCrMnFeCo). Model CSAs that we focus in this review include alloys from simple binaries (e.g. $\text{Ni}_{50}\text{Fe}_{50}$ (NiFe), $\text{Ni}_{50}\text{Co}_{50}$ (NiCo), $\text{Ni}_{40}\text{Fe}_{60}$, $\text{Ni}_{60}\text{Fe}_{35}$, $\text{Ni}_{80}\text{Fe}_{20}$, $\text{Ni}_{80}\text{Pd}_{20}$ and $\text{Ni}_{80}\text{Cr}_{20}$) and ternaries (e.g. $\text{Ni}_{33}\text{Co}_{33}\text{Fe}_{33}$ (NiCoFe), $\text{Ni}_{33}\text{Co}_{33}\text{Cr}_{33}$ (NiCoCr) and $\text{Ni}_{40}\text{Fe}_{40}\text{Cr}_{20}$) to more complex quaternaries (e.g. $\text{Ni}_{25}\text{Cr}_{25}\text{Mn}_{25}\text{Co}_{25}$ (NiCrMnCo), $\text{Ni}_{25}\text{Cr}_{25}\text{Fe}_{25}\text{Co}_{25}$ (NiCrFeCo) and $\text{Ni}_{25}\text{Mn}_{25}\text{Fe}_{25}\text{Co}_{25}$ (NiMnFeCo)) and quinary HEAs of NiCrFeCoPd and NiCrMnFeCo. To avoid confusion, the CSAs with equiatomic composition will be denoted only by the corresponding element symbols, as indicated in parentheses.

Of central importance for this set model alloys shown in **Fig. 1**, achieved by randomly replacing Ni atoms with various metal species at different concentration, is that these alloys form at equiatomic composition or high concentration, yet crystallize in fcc solid solutions with a high degree of chemical inhomogeneity. In these alloys, the random arrangement of multiple elemental species on a crystalline lattice results in the lack of long-range order or translational periodicity, in some extreme cases lack of short-range order as well. Since these alloys span a broad spectrum of substitutional disorder, it is therefore possible to understand how electron, phonon, and magnon systems are impacted by modifying chemical complexity; substantially reduce electron, phonon, and magnon mean-free paths; modify

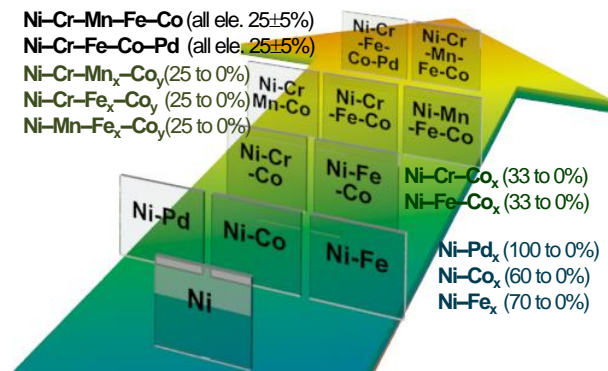


Fig. 1 Tunable CSAs where the range of possible variation for certain elements within the solid solution is noted in brackets. Extreme chemical disorder by altering alloy composition may pave the way for new design principles of functional alloys for energy applications.

1 coupling strengths; and create complex defect formation energy and migration barrier landscapes. Two
2 distinctive intrinsic properties are expected: (1) disordered local chemical environments that significantly
3 enhance electron-electron interactions and affect energy dissipation [2,12,15,16], and (2) unique site-to-
4 site lattice distortions that lead to atomic level compressive or tensile stress and complex energy
5 landscapes, which affect defect migration [12-14,22,23] and exceptional mechanical properties [3,10,11].

6 To quantify the first distinctive property, experimental and modeling studies have been carried
7 out on alloy systems with increasing chemical disorder (pure Ni metal and alloys of NiCo, NiFe, NiCoFe,
8 NiCoCr, NiCoCrFe, NiCoCrFeMn and NiCoCrFePd) to understand effects of compositional disorder on
9 the electronic structure, electron mean free paths, short-range order, and magnetic moments [2,12,15,16].
10 *Ab initio* Korringa-Kohn-Rostoker Coherent-Potential-Approximation (KKR-CPA) calculations [41] are
11 used to describe the ground state electronic and magnetic structure, and to reveal the effects of chemical
12 disorder on the underlying electronic structure. The results show that the Bloch spectral functions display
13 two characteristic features: little disorder in the majority states in the alloys containing only ferromagnetic
14 elements such as NiCo, NiFe, NiCoFe, and significant smearing in both minority and majority states in
15 alloys NiCoCr and NiCrFeCo where ferromagnetic Ni, Fe, and Co couple antiferromagnetically with Cr
16 [2,12,16]. A significant reduction of electrical and thermal conductivity of SP-CSAs is predicted for the
17 alloys with mixed ferro- and anti-ferromagnetic interactions, and is confirmed with electrical resistivity
18 and thermal conductivity measurements. Substantial electronic-level modification and significant
19 reduction of energy dissipation through coupled electronic and magnetic subsystems in these model alloys
20 are discussed and summarized elsewhere [2,12,16].

21 In this review, we focus on the second distinctive property to reveal the role of chemical
22 complexity on atomic processes – effects of atomic level disorder on energy landscapes. Most of the
23 standard conceptual tools for traditional alloys implicitly assume that the system is close to a periodic
24 solid. For example, vacancy and interstitial motion models assume that most of the lattice is
25 homogeneous with the same activation energies with the presence of discrete trapping sites in dilute
26 alloys due to minor alloying elements or lattice imperfections. Modeling CSAs requires the development
27 of new theoretical constructs and effective assembling techniques. While formation and migration
28 energies have been studied in ordered Ni metal, the effects of compositional disorder are unclear. In the
29 concentrated solid solutions, the traditional electron band theory, phonon transport and diffusion
30 implicitly applied to a system nearly periodic may fall apart. The symmetrically variation of elemental
31 species, composition and local disorder provides unique controls to understand defect physics (defect
32 energetics and complex energy landscape unique to CSAs) that may lead to radiation resistance.

33 34 **3B. Defect Energetics Unique to CSAs**

35 To understand the effects of random site occupancies of different elemental species, atomic-scale
36 properties resulting from lattice distortions of the fcc concentrated alloys are characterized. The atomic-
37 scale properties, such as point defects, rely greatly on their local environments. In particular, the
38 properties of defects are greatly affected by the chemical inhomogeneity presented in these CSAs [42].
39 The disorder comes from both the chemical disorder induced by random arrangement of different
40 elements (no element has the same neighbors) and the displacement fluctuation (lattice distortion) caused
41 by the different characteristics of elements. Such disorders cause the environment-dependent energetics of
42 defect formation and migration to be fundamentally different from pure materials and traditional dilute
43 alloys. As a result, the formation and migration energies of vacancies and interstitials have a distribution,
44 rather than having a single value as is generally thought in the dilute alloys. While the formation energy
45 measures the difficulty to create the defect, and the distribution in CSAs suggests that the defect could
46 exist over a large energy range. Moreover, the distribution of migration barriers will change the diffusion
47 mechanism of these defects. In addition, it is highly likely that the distribution of different kinds of
48 defects will overlap, which governs the degree to which the defect populations may separate. For
49 example, an overlap in the distribution of migration energies indicates similar diffusion coefficients and
50 thus a prolonged interaction time between different kinds of defects.

1 Although *ab initio* calculations have become standard methods to investigate the defect energies,
 2 the disorder in these CSAs possess great challenges to such modelling efforts. Two methods can be used
 3 to tackle the disorder presented in these systems. One is the coherent potential approximation (CPA)
 4 method [2,15,41] that is a single-site, mean-field theory capable of describing the composition disorder,
 5 including configurationally averaged single-site charge density, magnetization density, density of states,
 6 and total energy. However, the CPA method does not allow consideration of the effects of local lattice
 7 distortion or displacement fluctuations. While defects can be modeled as an additional (dilute) species, the
 8 distribution of formation energies and migration energies that results from local environmental effects
 9 cannot be obtained using the CPA method. In addition, it cannot be utilized to study the migration of
 10 defects due to its fixed lattice sites. The other approach is the supercell approach by constructing the
 11 special quasi-random structures (SQS) [43] that considers the structure details by relaxing the position of
 12 atoms, though the computational cost is much higher due to the large supercell required to simulate the
 13 defect properties. In this method, the effects of configurational averaging are often ignored as this
 14 information is assumed to be included in the SQS structure. Nevertheless, the supercell models provide
 15 detailed information about the defect structure, and thus are suitable for describing the distribution of
 16 defect energies.

17 Classical molecular dynamics (MD) and atomistic Monte Carlo (MC) methods based on
 18 interatomic potentials are on the other hand able to consider the disorder by computing plenty of
 19 structures and obtain configurational averages due to their much lower computational cost than DFT. In
 20 addition, it can be used to study the long-term evolution of defects at different temperatures. The defect
 21 evolution predicted by these potentials is closely
 22 related to the atomic-scale defect energies, since these
 23 energies determine the relative stability of different
 24 defects. For example, a high diffusion coefficient is
 25 always observed for the defects with lower formation
 26 energies, as they provide the diffusion channel to
 27 facilitate the defect migration. Since MD results
 28 depend sensitively on the interatomic potential used, it
 29 is therefore critical to validate the reliability of the
 30 potentials for predicting defect evolutions.

31 *Ab initio* calculations based on supercell
 32 method with a 108-atom SQS cell have been employed
 33 to characterize the distribution of defect formation and
 34 migration energies in CSAs [42]. In pure Ni, there are
 35 six possible interstitial configurations, i.e. octahedral,
 36 tetrahedral, crowdion as well as [100], [110] and [111]
 37 dumbbells. Among them, the [100] dumbbell is the
 38 most stable interstitial configuration with the lowest
 39 formation energy of 4.27 eV. The results for NiCo,
 40 NiFe, Ni_{0.8}Fe_{0.2} and Ni_{0.8}Cr_{0.2} show that the formation
 41 energies for vacancies are mostly higher than in pure
 42 Ni, while those for dumbbell interstitials are lower than
 43 in pure Ni (4.27 eV). The distribution of migration
 44 energies for vacancies and interstitials to overlap
 45 with increasing disorder from Ni_{0.8}Fe_{0.2} to NiFe,
 46 suggesting an unexpected equal mobility in the solid
 47 solution phase. This effect is the most prominent for
 48 NiFe, suggesting that the replacing Ni with Fe to form
 49 solid solution may have a notable influence on the
 50 defect energetics. Significantly enhanced irradiation
 51 resistance is reported from the ion irradiation

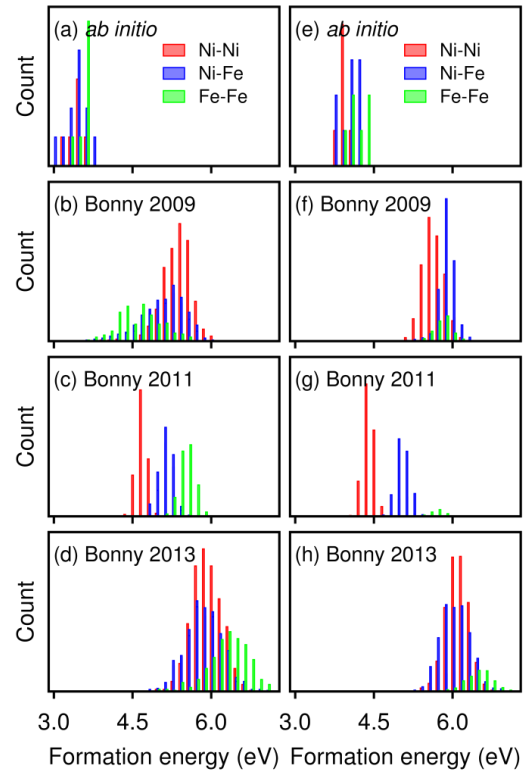


Fig. 2 Formation energy of a [100] dumbbell in NiFe (left column) and Ni_{0.8}Fe_{0.2} (right column) determined from *ab initio* calculations (a and e) and three EAM potentials: Bonny2009 (b and f), Bonny2011 (c and g) and Bonny2013 (d and h). There are 26 data points in the *ab initio* results. Adapted from Fig. 2 in Ref. 42

1 experiments for NiFe compared with pure Ni and NiCo [2,12], which indicates a potential link from
2 modified defect energetics to radiation performance. The *Ab initio* calculations also suggest that diffusion
3 barrier of interstitials in Ni_{0.8}Cr_{0.2} is found to be smaller than that in NiFe and Ni_{0.8}Fe_{0.2}, an indication of
4 faster migration of interstitials in Ni_{0.8}Cr_{0.2}.

5 The *ab initio* results for interstitial dumbbells in NiFe and Ni_{0.8}Fe_{0.2} are provided in **Fig. 2**,
6 together with the results calculated from three embedded atom method (EAM) potentials developed by
7 Bonny *et al.* [44-47]. To distinguish different versions, these potentials are denoted by the year they were
8 developed, as Bonny2009 [44], Bonny2011 [45], and Bonny2013 [46]. The results from the EAM
9 calculations are determined from a 2048-atom supercell to obtain a full sampling of the local
10 environments of dumbbells. The dumbbell is introduced at each site, and the dumbbell structure is picked
11 out after relaxation to calculate the formation energies. The results show that the formation energies from
12 the *ab initio* calculations are relatively small in both NiFe and Ni_{0.8}Fe_{0.2}. However, all three EAM
13 potentials predict larger formation energies with different distributions. The formation energy of the Fe -
14 Fe dumbbell is the largest for Bonny2013. Moreover, Bonny2011 results in three separate distributions
15 for the Ni-Ni, Ni-Fe, and Fe-Fe dumbbells, whereas Bonny2009 and Bonny2013 give largely mixed
16 formation energies. In NiFe, while the formation energies for Fe-Fe dumbbells are smaller from
17 Bonny2009 as compared to the Ni-Ni and Ni-Fe dumbbells, an opposite trend is observed from
18 Bonny2013. Compared with the *ab initio* results, Bonny2013 generates a similar distribution for all
19 dumbbells, although their energies are highly overestimated. It is worth noting that the small supercell
20 (108 atoms) used in the *ab initio* calculations tends to overestimate the formation energies of interstitials
21 due to the possible interactions between the interstitial and its periodical images. The smaller formation
22 energies of interstitials in NiFe are, therefore, not affected by the choice of supercells.

23 The diffusion barrier is calculated from Nudged elastic band (NEB) method. The migration of Ni
24 vacancies has a lower energy barrier than the migration of Fe vacancies, by hopping among the lattice
25 sites through exchange with Ni or Fe atoms, respectively, in both NiFe and Ni_{0.8}Fe_{0.2}. For interstitials, it is
26 found that Ni_{0.8}Cr_{0.2} has smaller diffusion barriers for Ni and Cr interstitials compared to NiFe and
27 Ni_{0.8}Fe_{0.2}. The migration energy in NiFe and Ni_{0.8}Fe_{0.2} is larger than that in pure Ni, which will give rise to
28 slow diffusion of interstitials in these two alloys. An important finding is that the migration energies of
29 vacancies and interstitials in NiFe have a region of overlap. The overlapping may greatly enhance defect
30 annihilation in NiFe and make it more resistant to ion irradiation [12].

31 The defect energetics discussed so far is basically obtained at 0K by neglecting the temperature
32 effect. Although it provides important insight into the particular feature of defect properties in CSAs, the
33 defect behaviors are likely to be affected by lattice vibration arising from finite temperatures.
34 Unfortunately, it is extremely computationally costly to address the vibrational properties by *ab initio*
35 calculation, as it requires accurate phonon calculations. Moreover, the activation energies for defect
36 diffusion are also temperature dependent. In this case, MD simulations that allow the consideration of
37 both temperature and local energy profiles are especially important.

38 39 **3C. Complex Energy Landscape Unique to CSAs**

40 In the NEB calculations, the diffusion barrier is calculated from the energy landscape by fixing
41 the initial and final state. This is useful when the initial and final state can be defined accurately.
42 However, these states are hard to be determined in actual irradiation environment that is far from non-
43 equilibrium condition. The problem can be solved by means of molecular dynamics simulations, in which
44 the defect is allowed to find its own migration pathway according to local environment and energy
45 landscape. Both *ab initio* molecular dynamics (AIMD) and classical MD simulations can be used, in
46 principle, to study the diffusion properties at finite temperature. However, as revealed from static NEB
47 calculations, the diffusion of defects in these CSAs is more difficult than in pure Ni. As a result, much
48 longer simulation time is required so that a large number of defect jumps is counted to capture the long
49 range diffusion behaviors in CSAs. This is a great challenge to MD simulations, especially for an AIMD,
50 which requires a high computational cost.

1 The diffusion of interstitials in NiFe, NiCo and NiCoCr is studied by AIMD within a 108-atom
2 supercell plus an interstitial. The typical simulation time is about 30 ps. In order to speed up the diffusion
3 process, different temperatures up to 1800K have been employed. Due to the sluggish diffusion in these
4 CSAs, the number of defect jump observed in such a short time scale is in the range of 300-1000
5 dependent on temperature. Most of the jumps for interstitials occur in the form of dumbbells along the
6 direction of $[1/2, 1/2, 0]$. The tracer diffusion coefficients are extracted from the calculated mean squared
7 displacement (MSD). The results suggest higher diffusion coefficients of Ni in NiFe, Co in NiCo, and Co
8 in NiCoCr. Detailed analysis indicates that the interstitials in these materials diffuse in the form of
9 specific dumbbells: Ni-Ni and Ni-Fe in NiFe; Ni-Co and Co-Co in NiCo; Co-Cr in NiCoCr. This is
10 closely related to their formation energies. As displayed in **Fig.2**, *ab initio* results show that Ni-Fe and Ni-
11 Ni dumbbells have lower formation energies than Fe-Fe. Therefore, the diffusion of interstitials in NiFe is
12 mainly through the Ni channel that leads to higher diffusion coefficient of Ni. Similar arguments are also
13 applicable to NiCo and NiCoCr. It seems that these systems all have distinguishable formation energy
14 distributions for different dumbbells. As a result, there is always one type of dumbbells that dominates in
15 these CSAs. This explains a preferable diffusion of a corresponding species. In fact, these observations
16 can be traced back to the structure of CSAs. In NiFe, it is found that the first nearest neighbor distance is
17 the largest for Fe-Fe, suggesting that Fe has larger radius than Ni in *fcc* NiFe. Ni-related dumbbells,
18 therefore, exhibit lower formation energies and preferable diffusion. The structural analysis for NiCo and
19 NiCoCr also predicts the same trend. Although this property is element-dependent, the preferable
20 diffusion provides evidences to modulate the distribution of formation energies and thus manipulate the
21 interstitial flow in various CSAs by tailoring their chemical complexities.

22 Mass transport is essential to materials performance, such as elemental segregation, phase
23 stability, thermal aging, mechanical stress, and radiation performance. In CSAs, while the properties of
24 defects are expected to be greatly affected by the chemical inhomogeneity (Section 3B), the complex
25 energy landscapes are anticipated to affect mass transport mechanisms and pathways. Classical MD can
26 extend to very long simulation time compared to AIMD, and it is widely used to study mass transport.
27 Most previous studies focus, however, on conventional dilute alloys, barely different from a pure element
28 material from the viewpoint of compositional complexity. Mass transport in CSAs has not drawn
29 sufficient attention until recently valuable information of interstitial and vacancy transport mechanisms is
30 obtained in NiFe [22] from long timescale simulations. The most striking finding is that vacancies and
31 interstitials in NiFe migrate through different alloy components. Comparing in Ni, the results in NiFe
32 indicate that replacing Ni with Fe, alloy chemistry leads to sluggish diffusion and elemental segregation.
33 It is found that the diffusion frequency in the equiatomic binary alloy is reduced significantly relative to
34 the pure Ni metal. In the binary alloy, interstitials move via Ni sites, while the vacancies primarily hop
35 among the lattice sites through exchange with Fe atoms. The results will allow prediction of segregation
36 behavior under thermal aging, where vacancy sinks are depleted, as Fe flows in the opposite direction to
37 vacancies. Moreover, it is also argued that Fe depletion near interstitial sinks will be significantly
38 enhanced by Ni enrichment under irradiation where interstitials and vacancies are produced directly. Such
39 modification of transport pathways is an important feature in concentrated alloys, including HEAs. The
40 work [22] points out that the Fe migration path should be broken, inhibiting vacancy diffusion if the Fe
41 concentration is below the fcc site percolation level of ~ 21 at%. Likewise, interstitial diffusion may
42 switch off when the Ni migration path is blocked with decreasing Ni concentration locally. In addition, by
43 introducing additional alloying elements into the migration pathways, it is expected that both the Fe and
44 Ni contiguous paths may be close that both vacancy and interstitial diffusion can be significantly
45 suppressed. An implication is that manipulating the chemical complexity may enable one to separately
46 affect interstitial or vacancy diffusion.

47 **4. Defect dynamics and irradiation performance of concentrated solid-solution alloys**

48 **4A. Materials response to radiation energy deposition**

1 The evolution of radiation-induced defect
2 concentrations can be described in simplified terms by three
3 competing processes: the 1st term containing defect
4 production from collision cascades; the 2nd term containing
5 subsequent vacancy-interstitial recombination within the
6 diffusion volume during the cascade events; and the 3rd term
7 including extended defect clusters formed from the
8 accumulation of the cascade damage within the host matrix,
9 as well as absorption by nano-scale features such as
10 additional phases, interfaces, grain boundaries, and
11 precipitates. Both the 1st and 2nd terms in such a simplified
12 description are short-time processes up to a few picoseconds
13 (the ballistic phase shown in Fig. 3), while the 3rd term
14 includes the processes over a much longer time scale (the
15 kinetic phase illustrated in Fig. 3 and much longer time
16 processes).

17 A collision cascade can be viewed as an ultra-fast
18 phase transition with complex thermodynamic and kinetic
19 behavior. The incoherent, high-energy motion of atoms in a
20 collision cascade affects the transport of vacancies and interstitials, both are expected to be strongly
21 influenced by the local energy landscapes. Random site occupancies and associated lattice distortions can
22 create large fluctuations of the lattice potential between different lattice sites that modify atom diffusion.
23 Such effects may be utilized hypothetically to suppressed defect production, resulting from enhanced
24 recombination of interstitials and vacancies created from cascade events (integration of 1st and 2nd terms).
25 Due to the extreme chemical disorder and lack of long-range ordering in complex CSAs, the energy
26 landscape will be highly heterogeneous and new theoretical approaches are needed.

27 It has long been observed that, compared to their pure metal counterparts, traditional alloys with
28 specific compositions have improved radiation resistance, as reviewed in Section 2, and recent research
29 on radiation damage mitigation has focused on the 3rd term through the introduction of a large number of
30 inhomogeneities at nanometer and micrometer level, such as oxide dispersion strengthened (ODS) steels
31 or layered structures. Lack of fundamental understanding of electronic and atomic level mechanisms in
32 the first two terms, as well as evolution of extended defects in the 3rd term due to the complex potential
33 energy landscapes in CSAs, hinders the possibility to design materials intrinsically resistant to radiation
34 damage. It is highly desirable to take advantage of property enhancements of concentrated alloys to
35 extrapolate beyond our knowledge from traditional alloys, by tuning chemical disorder, to design alloys
36 intrinsically resistance to radiation damage. Meeting this challenge demands an understanding of the role
37 of each constituent element and the composition complexity, so that ultimately it is possible to suppress
38 primary defect production and delay damage accumulation in extreme radiation environments.

39 Enhancement of radiation tolerance performance in CSAs is different from approaches in
40 traditional dilute alloys relying on altering minor elements or modifying microstructures, one hypothesis
41 is to modify alloy complexity to control defect dynamics at the early stage of radiation damage, and
42 ultimately reduce surviving defect concentrations and enhance radiation tolerance at a later stage. In other
43 words, by tuning chemical complexity to control energy dissipation and defect evolution, it may be
44 possible to significantly reduce the number of surviving defects (the 1st and 2nd terms). Simultaneously,
45 defect dynamics and various energy dissipation processes can be similarly tuned to be more localized,
46 thus enhancing defect absorption at the extended defects and consequentially forming less undesirable
47 damage (processes involved in the 3rd term). Such modified processes (<http://edde.ornl.gov/>) would delay
48 damage accumulation and lead to more intrinsically radiation-robust alloys.

49 The tunable chemical complexity, the static defect energetics and transport properties, and
50 complex energy landscapes were reviewed in Section 3. In this section, possible effects of chemical
51 complexity to minimize the 1st term, maximize the 2nd term, and modifying the 3rd term are discussed. The

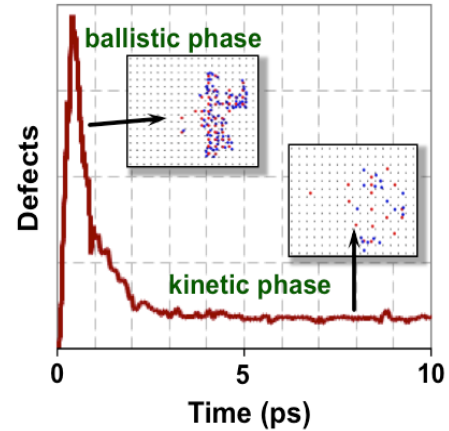


Fig. 3 Schematically showing generation of point defects forming a peak during the ballistic phase followed by vacancy-interstitial recombination during the kinetic phase leaving behind few surviving defects.

1 discussions focus on the non-equilibrium defect kinetics during and after the cascade collisions, as well as
2 during a long-term accumulation.

3 4 **4B. Defect production and damage accumulation**

5 Recent advances have shown possibilities of controlling defect dynamics at their early stages,
6 including both ballistic phase and kinetic phase, as schematically shown in **Fig. 3**, by changing the
7 compositional complexity of CSAs. Modeling activities, advancing quickly, have benefitted from the
8 availability of comprehensive knowledge and high-performance codes. *Ab initio* theory, time-dependent
9 density functional theory (TD-DFT), AIMD, and classical MD simulations have revealed how alloy
10 complexity can alter energy dissipation (the first distinctive property described in Section 3A) in the
11 electronic and atomic subsystems [48-51], thereby offering the possibility of enhanced defect
12 recombination or self-healing radiation resistance. Increasing experimental activities are evident in recent
13 literatures [2,12-14,23], including the successful growth of large single crystals, the integrated
14 experiments and modeling predictions [2,12,13,52-57], and the collaborative execution of well-defined
15 irradiation experiments and microstructural characterization to evaluate compositional effects on radiation
16 response [12-14,17,23,55-59].

17 18 **4B-1. Computational challenges and approaches developed**

19 Modern materials science relies heavily on using a multiscale combination of computational
20 methods to study both equilibrium and nonequilibrium effects. With respect to phase stability and defect
21 properties, quantum mechanical density functional theory (DFT)-based first principles calculations are
22 advanced to examine the relative energetics and determine defect formation energies in CSAs (see
23 Section 3B) [60]. They can also be used to provide the necessary inputs for constructing classical
24 interatomic potentials to carry out MD (see examples in Section 4B-2) or Metropolis Monte Carlo
25 (MMC) simulations, which can be used to simulate atom dynamics and thermodynamic properties,
26 respectively. MD simulations are, however, limited to nanosecond time scales, while MMC does not
27 have a time scale at all. To access longer time scale processes, e.g. defect migration, kinetic Monte Carlo
28 (KMC) methods may be used. The required inputs, such as defect migration rates, can, at least in
29 principle, be obtained from DFT and/or MD simulations.

30 For concentrated solid solution alloys, the use of all these techniques has particular challenges. In
31 DFT, which is limited typically to a few hundred atoms, as noted above it becomes difficult to obtain a
32 representative sample of atom configurations due to the necessity to mix atoms of many types in many
33 different configurations. Classical MD or MMC simulations, on the other hand, require as the crucial
34 physics input of interatomic potentials. These are usually constructed by fitting a relatively simple
35 functional form or set of cubic spline nodes into a set of experimental and DFT data of different phases
36 with possible elastic, defect and surface properties. However, for CSAs so far little experimental data is
37 available, and the difficulties on carrying out DFT calculations also hamper the setup of generating inputs
38 for MD. Also, it is not obvious into which kind of configurations and with what procedure to fit all the
39 mixed-element interactions. Finally, for setting up KMC simulations, one would need in principle to
40 know defect migration rates for all possible atomic configurations forming a defect. To illustrate the
41 complexity of this, one can consider just the simplest possible defect, a single vacancy. Such a vacancy in
42 an fcc crystal is surrounded by 12 neighbors, and hence in a high-entropy alloy of 5 elements has 5^{12}
43 possible surrounding configurations. Even with current computer capacity, tabulating this number of
44 configurations is practically impossible, and hence other methods, such as on-the-fly barrier calculations,
45 need to be used.

46 Notwithstanding these challenges, progress has been made on developing simulation techniques
47 for CSAs on all the simulation levels, especially advances in *Ab initio* calculations as discussed in Section
48 3B and MD simulations in Section 4B-2 and 4B-3. In the following, we briefly review some of these
49 approaches that are uniquely applicable to CSAs.

50 51 **4B-2. Development of interatomic potentials**

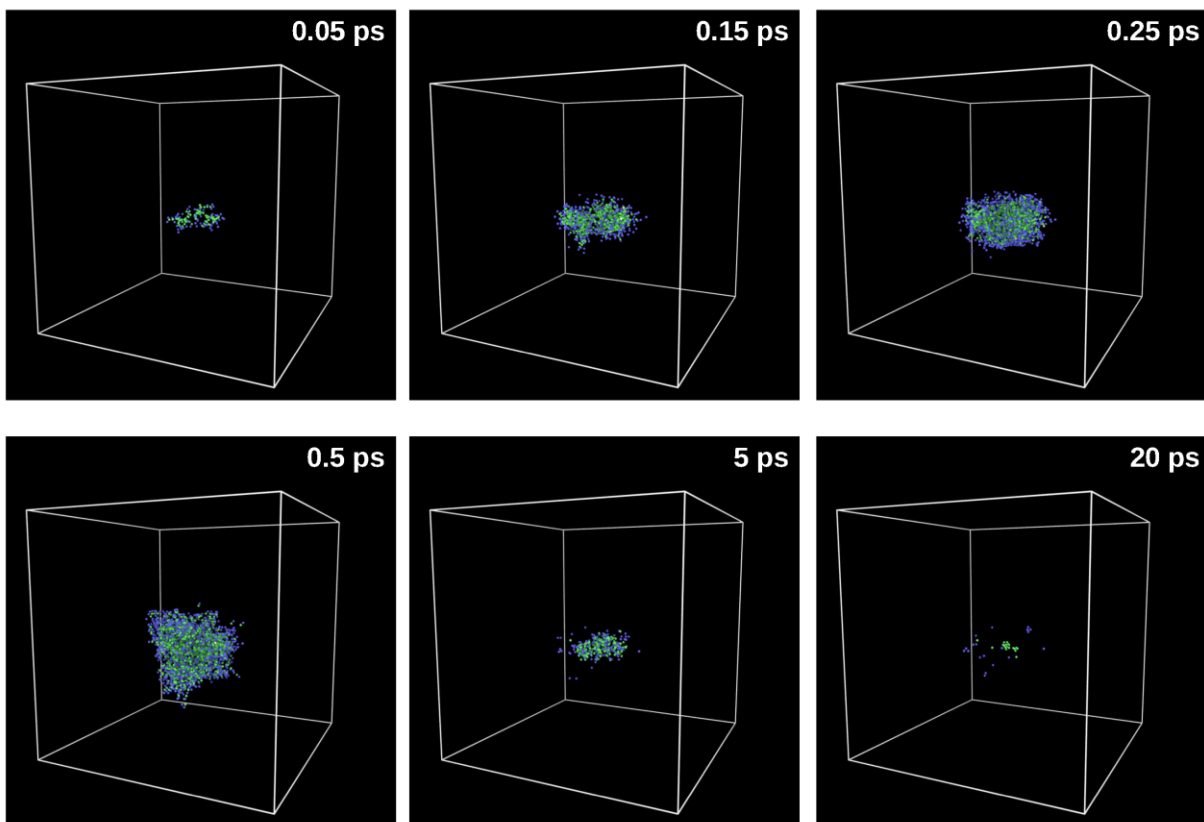


Fig. 4 Defect formation in a 10 keV self-recoil induced cascade in NiCrFeCo. The green spheres indicate the position of vacancies and the purple ones are the interstitials. The white box shows the entire simulation cell.

1 Cascade events often produce many interstitials and vacancies. To assess defect dynamics,
 2 atomistic simulations with empirical interatomic potentials are a common approach. Recent MD work
 3 [61-63] has identified a problem of short-range forces in radiation damage modeling. In **Fig. 2**, the
 4 *ab initio* results in the Ni-Fe alloys are compared to those calculated from available empirical interatomic
 5 potentials [44-47], and the results indicate that these empirical potentials are insufficient to describe the
 6 energetics of interstitials in Ni-Fe alloys. For examples, the results from the 2013 Bonny potentials show
 7 that replacing Ni with Fe decreases primary damage production, consistent with experimental
 8 observations [2,12], while using the 2009 Bonny potential leads to an opposing conclusion – increase in
 9 damage production. The issue is attributed to difference in the interatomic potentials at short interatomic
 10 distances that are typically inaccurately modeled [62,63].

11 In displacement cascades, extreme pressures and temperatures arisen from the high-energy
 12 recoils, bringing atoms closely together where the interatomic distances become very short, $\sim 1-2 \text{ \AA}$. At
 13 such distances, the interatomic interactions are poorly described by most interatomic potentials commonly
 14 used for atomistic modeling. [62,63]. Atomic level interactions at larger separation distances are
 15 controlled by the equilibrium properties of the material, which are used to parameterize the interatomic
 16 potentials to ensure reliable results of atomistic simulations in near equilibrium conditions. The common
 17 practice is to transition from the equilibrium potential to the repulsive universal potential by Ziegler,
 18 Biersack, and Littmark (ZBL) at small atomic separation distances.

19 During the early phase of collision cascades, the interatomic separation of the two colliding atoms
 20 can be much smaller than the equilibrium lattice parameter, and the interatomic potentials fitted to
 21 equilibrium properties tend to significantly underestimate the potential energy of the colliding dimer.
 22 Recent studies [61-65] identify this significant and yet underappreciated issue in joining the equilibrium

1 potentials to the ZBL potential. Different
 2 approaches with an arbitrary function within an
 3 arbitrary region of space are commonly used for
 4 such a transition, which may result in an
 5 unphysical prediction. The lack of a unified
 6 approach to describe the joining to short-range
 7 forces may be problematic for comparing defect
 8 production between different potentials.

9 Several *ab initio* based methods have
 10 been utilized to calculate short-range interactions
 11 of atoms, including those in high-pressure states
 12 [63,65]. Accurate representation of the forces
 13 involved is possible by refitting classical
 14 interatomic potentials. The recent work has
 15 demonstrated that using first-principles
 16 techniques it is possible to accurately describe
 17 the energy of interatomic interactions in this
 18 transition region and the atomic collisions taking
 19 place within the short interatomic distances play
 20 a significant role in determining survival primary
 21 damage production. These recent studies [61-63]
 22 indicate that the development of potentials for
 23 CSAs is essential.

24 4B-3. Primary damage formation from cascade event within the ballistic phase

25 Molecular dynamics simulations have been used extensively to understand the time dependence
 26 of damage production in collision cascades [13,53,62,63] induced by keV-energy ions or recoils. These
 27 simulations consistently show that in metals, there is violent damage production initially by ballistic
 28 collisions (**Fig. 3** ballistic phase), which in turn lead to formation of a so-called heat/thermal spike.
 29 However, after a few ps, much of the damage recombines during the kinetic phase and much longer time
 30 evolution. In metals, this relaxation effect is particularly strong, leading to a reduction in number of
 31 defective atoms of about two orders of magnitude (see **Figs. 4** and **5**). The results in **Fig. 5** were obtained
 32 with the interatomic potentials of Zhou et al [66]. The underlying mechanism is that pure metals have a
 33 very strong capability to recrystallize. In semiconductors and insulators, the recombination effects are
 34 much smaller, roughly a factor of two due to the possibility to create amorphous damage pockets.

35 The picosecond time scale defect creation behavior that could be expected for high-entropy alloys
 36 is not *a priori* clear. Although pure metals do exhibit strong recombination, on the other hand many metal
 37 alloys can be made amorphous (becoming bulk metallic glasses), and these remain amorphous during
 38 irradiation, even exhibiting increasing degrees of disorder. Some simulations of collision cascades in
 39 concentrated solid solution alloys known to be stable experimentally do show consistently that the initial
 40 damage production in them (the 1st and 2nd terms) is very similar to elemental metals. This is illustrated in
 41 **Fig. 5**, which shows that the time dependence in Ni and NiFe is fairly similar, and the fluctuations
 42 between individual cascades is larger than the difference between the materials. Simulating the damage
 43 production systematically in 100 different single cascades showed that, at least in the interatomic
 44 potentials of Zhou et al [66], the damage production in the alloys is on average slightly higher than those
 45 in the pure element Ni. However, the difference is fairly small, within ~30% between Ni and the alloy
 46 that showed the highest damage (NiFe). Some studies of the damage production in individual cascades
 47 show that the number of remaining defects after the cascade cooling down phase in initially pristine
 48 lattice is practically identical, at least in the cases of Ni, NiFe, NiCo, NiCoFe and NiCoCr [13,53] the
 49 amount of defects (vacancies + interstitials) produced by a single 5 keV cascade in the corresponding
 50 pristine materials averaged among 100 PKA events. In other words, no damage reduction is observed in
 51

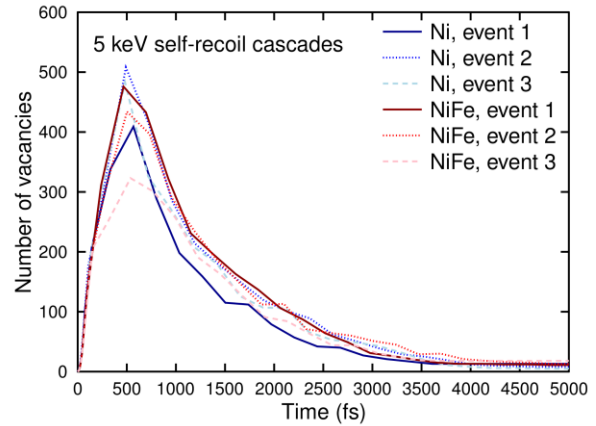


Fig. 5 Defects as a function of time in cascades induced by 5 keV self-recoils in bulk Ni and NiFe. Defects form a peak during the ballistic and heat spike phases of the cascade development, and follow by vacancy-interstitial recombination during the recrystallization phase leaving behind few surviving defects. For both materials, three different recoil events that differ only in the initial direction of the recoil are shown to illustrate the stochastic fluctuations in defect formation.

the 1st and 2nd terms. Hence the experimentally observed major differences between damage production in elemental solids and the concentrated solid solution alloys may be sought on longer-term development during the defect buildup or mobility phase (See Section 4C). It is worth pointing out that some studies [13] show no reduction on primary damage production at low fluences, others have indicated significant reduction [2,61,67].

Irradiation damage processes are conventionally simulated by giving a primary knock-on atom (PKA) kinetic energy that is dissipated through elastic collision events, where high PKA energies may lead to a cascade or a few sub-cascades of elastic scattering collisions. The evolution of such radiation-induced defects is the result of the production and instant recombination (1st and 2nd terms) as well as diffusion and accumulation of the defects over time that can be broken down primarily into two stages, i.e., ballistic stage (up to ~ 2ps) and kinetic stage (after a few ps), as shown in **Fig. 3**. A different approach has been applied to CSAs in MD simulations to study point defect interactions at very high concentrations [52, 54]. Instead of creating Frenkel pairs via time-consuming ballistic recoil events in MD cascade simulations as shown by the peak in **Fig. 3**, arbitrary concentrations of Frenkel pairs randomly distributed in a thermalized system can be introduced at the start of the simulation. This approach may be considered as being defect driven, with a focus on capturing the evolution of point defects, such as those created by low-energy ballistic events (e.g., electrons and protons), those that survive single or multiple cascade events, or those that survive a melt-quench process due to extreme electronic energy deposition along a high-energy heavy ion path. The advantage of the method is that relatively long MD simulation times can be achieved because the very short time steps required to simulate the high-energy ballistic defect production process are eliminated. In this approach, microstructure evolution is accelerated or driven by the larger Frenkel pair concentration. Relatively large vacancy and interstitial clusters can be obtained by the diffusion and aggregation of individual point defects [52, 54]. The disadvantage is that the processes inherent to more energetic ballistic events, such as the effects of shock waves [62,63], high displacement densities [67], and thermal spikes [67], which may affect defect production, are not captured. Also not captured are the concentrations or dose dependences of phase transformations, such as amorphization in ordered intermetallic compounds, or the slow evolution of microstructure when Frenkel pairs are added one-by-one with time.

MD simulations of high-energy Ni ion cascades (a few ten keV Ni ions) have been carried out in Ni and NiFe with and without consideration of electronic energy loss and e-ph coupling. The electronic effects are incorporated in the MD simulation using a two-temperature MD (2T-MD) model that couples

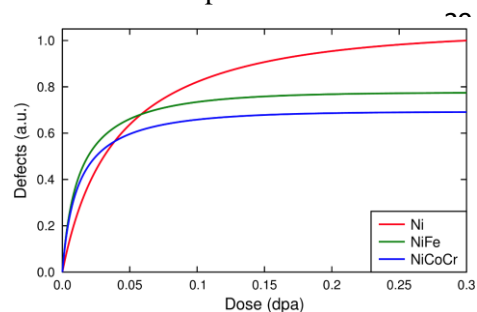


Fig. 7 MD results of damage accumulation in Ni, NiFe, and NiCoCr. The defects are scaled to the amount of defects in pure Ni.

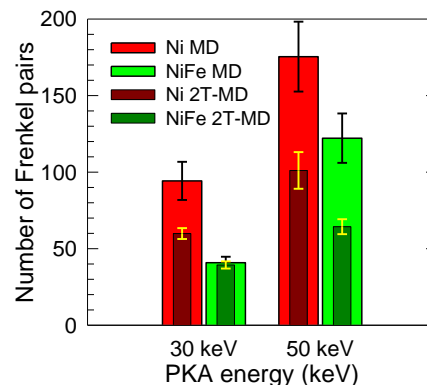


Fig. 6 Number of defects averaged over 12 PKA events (30 and 50 keV Ni), for classical MD simulations where kinetic energy is treated as nuclear energy loss, and for cascades where the electronic stopping is included in a 2T-MD model. The standard error is indicated. Adapted from Fig. 1 in Ref. 67.

the electronic and atomic subsystems based on their thermal transport properties (e-ph coupling parameter and specific heat) obtained from first principles calculations [67]. The results in **Fig. 6** illustrate the number of surviving defects (sum of interstitials and vacancies) at the end of the simulation time for 30 and 50 keV Ni cascades averaged over 12 events in Ni and NiFe. The predicted damage in NiFe is significantly lower than in Ni for both simulation approaches, opposite to the results from the 5 keV cascaded simulations as discussed earlier [13,53]. The effect of the electronic stopping is more profound in the higher energy cascades, and the energy returned to the lattice via the e-ph interactions enhances defect recombination, which is more evident in the 50 keV NiFe

1 case. The electronic interactions affect not only the amount of damage produced in the system, but also
 2 the way the defects are arranged into clusters. More isolated defects are predicted from the 2T-MD
 3 simulations.

4 It is demonstrated that electronic effects, especially at higher energies, can affect the damage level
 5 and the defect configuration. Reliable description on defect production from cascade events within
 6 picosecond timescale is of great importance to predict defect evolution and long-term performance, and
 7 research advances are highly desired to better describe short-range interatomic interactions, the quench of
 8 a collision cascade (therefore the degree of
 9 agglomeration of vacancies and interstitials), and initial
 10 conditions for subsequent microstructure evolution.

11 4B-4. Defect production and damage accumulation 12 during the kinetic phase

13 Computational work has provided insight into
 14 how compositional differences alter kinetic evolution of
 15 defect structures (3rd term) from overlapping cascade
 16 simulations [13,53]. Overlapping cascades by molecular
 17 dynamics is the most straightforward way to simulate
 18 damage buildup, i.e. running first the evolution of the
 19 development of one collision cascades, then taking the
 20 end result of this cascade as starting position for another
 21 running cascade. Since each MD cascade simulations is
 22 typically run on time scales of the order of 100 ps, and
 23 the simulation cell sizes are of the order of 10 nm, this
 24 approach will strongly overestimate the irradiation flux,
 25 and ignore thermal defect migration that occurs between
 26 cascades [13]. On the other hand, experiments
 27 comparing damage production at 30 and 300 K in
 28 metals showed fairly similar damage structures,
 29 indicating that such an approach nevertheless can be
 30 good as a first approximation to study damage buildup.

31 MD simulations at 300 K reveal significant
 32 differences in damage accumulation between pure Ni
 33 and the alloys of NiCo, NiFe, Ni_{0.8}Fe_{0.2} and Ni_{0.8}Cr_{0.2}
 34 that are consistent with ion channeling results showing
 35 slow damage accumulation in alloys. Simulations
 36 suggest that alloying elements modify the short-range
 37 interatomic interactions and reduce thermal conductivity
 38 [2,12]. Consequentially, chemical complexity may
 39 result in prolonged lifetime of the thermally enhanced
 40 recombination stage, suppress the formation of large
 41 extended defects in alloys due to more localized defect
 42 migration as they are not as energetically favorable as in
 43 Ni. Radiation-induced damage accumulation in
 44 Ni_{0.8}Fe_{0.2} and Ni_{0.8}Cr_{0.2} was compared with Ni using
 45 MD simulations based on the Bonny 2013 potential [46]
 46 to assess possible enhanced radiation resistance [53].
 47 The results show that the defect evolutions are
 48 remarkably different in Ni_{0.8}Fe_{0.2} and Ni_{0.8}Cr_{0.2} alloys
 49 than in the pure Ni system. The total number of point
 50 defects produced under the same dose in Ni_{0.8}Cr_{0.2} and
 51

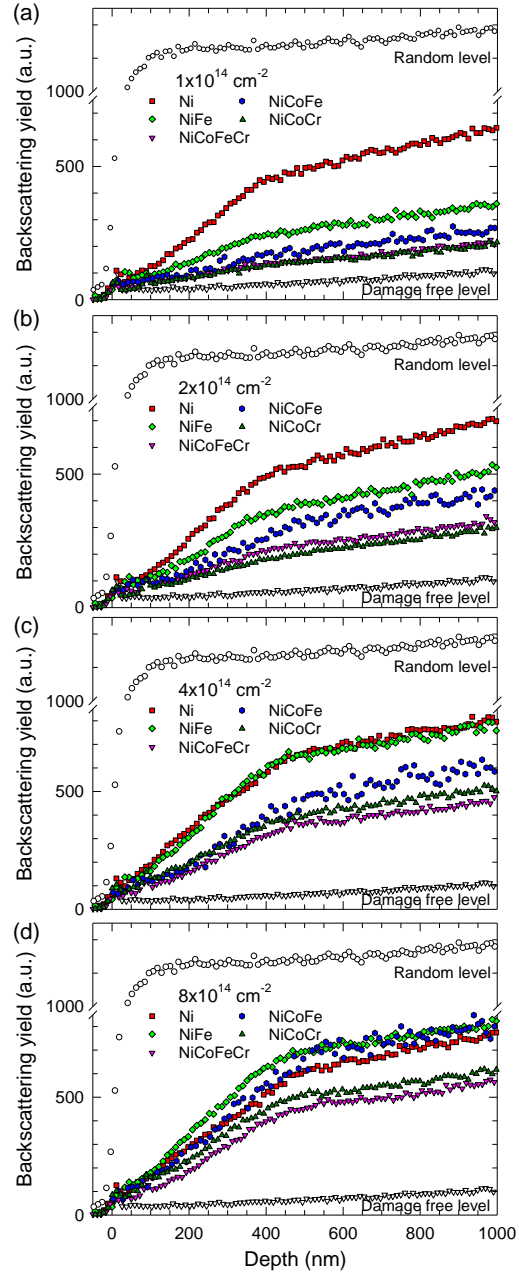


Fig. 8 Rutherford backscattering spectra along the (001) channeling direction. Different irradiation response in Ni and CSAs are observed under 1.5 MeV Ni irradiation at room temperature with fluences ranging from 1×10^{14} to $8 \times 10^{14} \text{ cm}^{-2}$.

1 $\text{Ni}_{0.8}\text{Fe}_{0.2}$ is approximately 2.5 and 1.4 times lower than
 2 in Ni, respectively, due to efficient recombination in the
 3 compositionally disordered alloys. The difference in
 4 defect production between the alloys and Ni is governed
 5 by the diffusion of point defects during overlapping
 6 cascades [22]. Although the formation of a large
 7 interstitial cluster is observed in Ni and is attributed to
 8 the high mobility of Ni interstitials, only isolated point
 9 defects and small clusters are produced in $\text{Ni}_{0.8}\text{Cr}_{0.2}$.
 10 While the larger fraction of small defect clusters in the
 11 binaries is attributed to the higher migration barriers and
 12 slow kinetics, the direct evidence is yet to be seen
 13 experimentally. Independent studies of overlapping
 14 cascades in Ni, NiFe and NiCoCr [13] also report a
 15 reduction of damage after prolonged irradiation (**Fig. 7**)
 16 that agreed qualitatively with the experimental
 17 observations [2,12,13]. The results were explained in
 18 terms of the multi-elemental composition in NiFe and
 19 NiCoCr slowing down dislocation motion, leading to
 20 slower buildup of large damage structures. Simulated
 21 defect buildup in Ni and two equiatomic alloys (**Fig. 7**) suggests that initially the alloys show a slightly
 22 higher damaging rate, but on higher doses the alloys have much less damage than pure Ni, also in
 23 qualitative agreement with the experiments. The evolution of microstructure in concentrated alloys under
 24 irradiation should be qualitatively different from that in dilute alloys, due to the significantly modified
 25 point defect diffusion and defect cluster mobility resulting from local chemical environment.

26 In order to investigate defect survival from multiple overlapping cascades at realistic fluxes, it is
 27 necessary to simulate defect evolution that occurs between the cascades. Accelerated aging approaches
 28 are establishing to describe such defect evolution after the initial picosecond timescale. Accelerated aging
 29 approaches based on calculating the barriers “on-the-fly” during a KMC run are being developed to
 30 describe defect evolution in the CSAs. The kinetic activation relaxation technique (k-ART) is an
 31 algorithm capable of simulating atomic systems over timescales reaching more than one second at RT,
 32 while accounting for off-lattice defects and elastic interactions [68]. To simulate the long-term aging of
 33 large disordered systems with cascade debris, this k-ART method has been recently modified [2,69],
 34 utilizing an active volume concept developed in an on-the-fly KMC [70], to describe significantly
 35 complicated system, such as CSAs. The original k-ART [68] can study systems containing up to a few
 36 thousand atoms, and the modified method [69] can efficiently simulate systems containing hundreds of
 37 thousands of atoms.

38 To understand effects of chemical complexity on defect evolution, recent successes in
 39 experimental work have provided crucial baseline information on improved irradiation response.
 40 Experimental evidence has demonstrated that defect dynamics can be modified by simply altering
 41 elemental species and composition of the CSAs. By changing from pure Ni metal to binary, ternary and
 42 quaternary alloys, a delayed accumulation can be achieved, as compared to Ni [2,12-14,17,23]. As shown
 43 in **Fig. 8**, different irradiation response is evident under 1.5 MeV Ni irradiation. The peak dose at depth of
 44 375 nm is $\sim 0.13, 0.27, 0.54,$ and 1.1 dpa for the ion fluence of $1, 2, 4$ and $8 \times 10^{14} \text{ cm}^{-2}$, respectively. At
 45 the relatively low doses ($1 \times 10^{14} \text{ cm}^{-2}$ and $2 \times 10^{14} \text{ cm}^{-2}$), significantly hindered damage accumulation is
 46 observed, as compared with pure Ni. As shown by the lower backscattering yield, NiCoCr and NiCrFeCo
 47 outperformed NiCoFe and NiFe. With increasing ion fluences to $4 \times 10^{14} \text{ cm}^{-2}$ and $8 \times 10^{14} \text{ cm}^{-2}$, while the
 48 most radiation-resistant alloys are still NiCoCr and NiCrFeCo, different saturation level is observed, and
 49 irradiation-induced damage moves deeper into the samples (**Figs. 8c and 8d**). Specific alloying effects
 50 responsible for these observed responses are topics for further investigation.

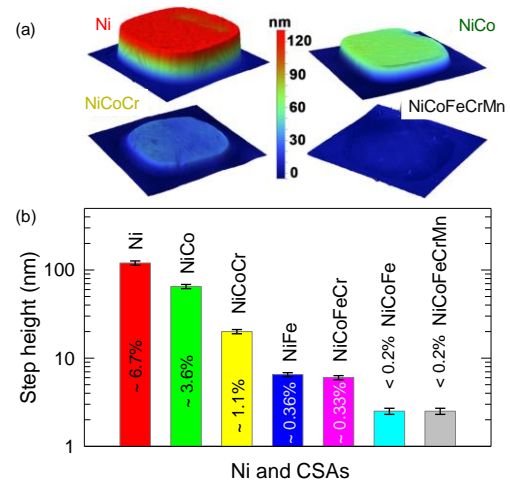


Fig. 9. Comparison of swelling between Ni and CSAs based on step height measurements, under 3 MeV Ni^+ irradiation to $5 \times 10^{16} \text{ cm}^{-2}$ at 500 °C. Adapted from Fig. 2 in Ref.17.

4C. Microstructural evolution under prolonged high-temperature irradiation

A major challenge in characterizing defect clusters and understanding defect evolution is to establish links among microscopic models, defect observations at early stages, and mesoscale phenomena (interstitial loops and void swelling) under prolonged defect evolution. Enhanced irradiation resistance at high doses and high temperatures is essential for advanced reactor applications. Recent studies [14,17] have shown significant compositional impact on defect evolution under Ni ion irradiation at 500 °C with a peak dose of ~

53 dpa at a depth of ~ 900 nm. A dramatic reduction of swelling in complex alloys is shown in **Figs. 9** and **10**. TEM irradiation study in **Fig. 10** reveals a colossal difference in swelling behavior and defect cluster distribution. *In-situ* observation of defect migration and MD simulations indicate that 1D glide of interstitial loops occurs more readily in Ni than in the alloys. As compared to NiFe and other more complex CSAs, the relatively long 1D migration path observed in Ni leads to less recombination of interstitials and vacancies. On the other hand, the more localized defect motion in NiFe and other more complex alloys leads to the remarkably enhanced defect recombination and substantial reduction in void formation and volume swelling. The defect diffusion in CSAs depends on the properties and diffusion mechanisms of specific defects in their unique environment. The results here show that chemical complexity can be used to modify void and dislocation loop distribution.

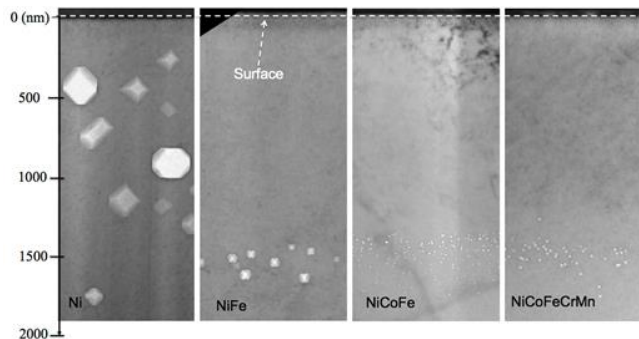


Fig. 10. Void formation in Ni and Ni alloys under 3 MeV Ni⁺ irradiation to $5 \times 10^{16} \text{ cm}^{-2}$ at 500 °C. More complex alloys exhibit smaller void formation, reducing swelling.

5. Perspectives— Chemical Effects and Atomic-level Heterogeneity on Irradiation Performance

To design better materials for energy technologies, a thorough understanding of the underlying physics and chemistry of simple and complex solid solution systems is essential to identify, understand and ultimately control the non-equilibrium energy and mass transform processes in extreme radiation environments. The local atomic arrangement and the corresponding energy landscapes of materials can be modified, which is of course not limited to metals and alloys. These chemical effects may lead to remarkable differences in resistance to radiation damage or amorphization.

Oxides with similar structure can exhibit different damage and amorphization behavior [71,72-74]. In the study of radiation tolerance of complex oxides, pyrochlore compositions display distinctive responses to ion beam-induced amorphization, depending on the chemical composition [72,75]. Pyrochlore materials, in the $A_2B_2O_7$ crystal structure, have remarkable elemental versatility. These changes in structure and chemical durability affect long-term performance of the actinide waste forms. Radiation studies of actinide-doped, synthesized or natural pyrochlores indicate that pyrochlores with Ti, Nb, and Ta as the major B-site cations become amorphous as a result of the gradual accumulation of cascade damage. With the increasing ionic radius of the A-site cation, from Lu^{3+} (0.098 nm) to Gd^{3+} (0.106 nm), the critical temperature for amorphization, above which the material will not be amorphized, increases from 480 K (for $\text{Lu}_2\text{Ti}_2\text{O}_7$) to 1120 K (for $\text{Gd}_2\text{Ti}_2\text{O}_7$) [76,77] under Kr^+ ion irradiation; however, the critical temperature for this material is nearly constant (1000 K) under heavy ion irradiation [78]. Zirconate pyrochlores are generally resistant to radiation-induced amorphization, and both $\text{Gd}_2\text{Zr}_2\text{O}_7$ and $\text{Er}_2\text{Zr}_2\text{O}_7$ remain crystalline at doses as high as 100 dpa at cryogenic temperatures [71,79]. Sickafus et al. [71] point out that fluorite crystal structure should accept radiation-induced defects into their lattices far more readily than a structurally similar pyrochlore crystal structure, therefore, fluorites are inherently more radiation resistant than pyrochlores. Sickafus et al. [71] have, however, proposed that complex oxides, which possess both complex chemistry and structure and therefore an inherent propensity to

1 accommodate lattice disorder, should be able to resist lattice instability in the presence of a displacive
2 radiation environment.

3 In contrast to Sickafus' hypothesis, Trachenko et al. [73] have suggested that the type of
4 interatomic force may hold the key to radiation performance. He proposes that the ability to form a short-
5 range covalent network leads to damage stabilization and makes a material amorphizable by radiation
6 damage. The long-range high ionicity, on the other hand, results in higher resistance. Such argument may
7 be supported by the fact that most metals and alloys where metallic bonding has even longer range are in
8 general radiation resistance. Examples supporting his argument in oxides include SiO_2 , TiO_2 , and GeO_2 .
9 Crystalline SiO_2 is easily amorphizable but TiO_2 is more resistant than SiO_2 and GeO_2 , which is attributed
10 to its larger ionicity in the bonding of TiO_2 than in the classical network formers SiO_2 and GeO_2 .
11 Trachenko has further demonstrated that complex titanates (such as perovskites CaTiO_3 , SrTiO_3 , BaTiO_3 ,
12 pyrochlores $\text{Gd}_2\text{Ti}_2\text{O}_7$, $\text{Sm}_2\text{Ti}_2\text{O}_7$, $\text{Eu}_2\text{Ti}_2\text{O}_7$, $\text{Y}_2\text{Ti}_2\text{O}_7$, zirconolite $\text{CaZrTi}_2\text{O}_7$), due to disordered covalent
13 Ti-O-Ti, are readily amorphizable by radiation damage. On the other hand, the binary oxides MgO , ZrO_2
14 and Al_2O_3 are known to be highly resistant to amorphization by radiation damage, which Trachenko
15 attributes the performance to the high ionicity of these binary oxides [73]. The same argument, high
16 ionicity of Zr-O bond, is used to explain the extreme resistance of zirconate oxides $\text{Gd}_2\text{Zr}_2\text{O}_7$, $\text{Sm}_2\text{Zr}_2\text{O}_7$,
17 $\text{Nd}_2\text{Zr}_2\text{O}_7$, $\text{Ce}_2\text{Zr}_2\text{O}_7$ and $\text{Er}_2\text{Zr}_2\text{O}_7$. Trachenko further proposes that the resistance to amorphization of a
18 complex (non-metallic) material is defined by the competition between the short-range covalent and long-
19 range ionic forces.

20 Another well-studied case of chemical complexity effects on radiation damage involves III-V
21 semiconductors. Due to their importance in optoelectronics, radiation damage in III-V semiconductors
22 have been studied extensively [80-84]. The case of $\text{Al}_x\text{Ga}_{1-x}\text{As}$ compounds is particularly intriguing, in
23 that it shows a drastic change in damaging behavior when only a small fraction of Al is used to replace
24 Ga. [85]. This is particularly surprising since during the addition of Al, the crystal structure remains the
25 same, and there are no drastic changes in lattice constant, band gap or any other basic materials property.
26 The sensitivity has been suggested to be related to higher defect mobility in AlAs [83], however, why the
27 effect occurs already at low Al concentrations has not been explained.

28 Chemical effects on resistance to amorphization are thus still an open research topic. Chemical
29 complexity can induce atomic-level stress that is not limited to only crystalline materials. Nearly 30 years
30 ago, well before the development of the HEAs, the concept of atomic-level stresses related to local
31 incompatibilities was argued as a general means for describing complex atomic structures [86]. The
32 authors state that only in perfect crystals in which all the atoms are equivalent, such incompatibilities do
33 not exist. Local incompatibilities are, however, present in ordered structures with non-equivalent atoms,
34 such as in CSAs [2], and in any disordered structure, such as in BMGs [87,88]. Egami in 2010 pointed out
35 [88] that major mysteries still remain in the behavior of glasses and liquids at the atomic level, and
36 identifying the microscopic mechanisms that control the properties of glasses is one of the most
37 challenging unsolved problems in physical sciences. He further stated that as metallic glasses are atomic
38 glasses with relatively simple structure, they may offer better opportunities to advance our fundamental
39 understanding on the nature of the glass transition. Recent studies investigate the variations of inherent
40 structures and properties with respect to the hopping between different local minimum states on a
41 potential energy landscape (PEL) in metallic glasses [89,90], a material system with a complex energy
42 landscape similar to CSAs. From the perspective of PEL, the authors demonstrate that the activation
43 energy spectra consistently change at varying thermal environments, and PEL structures are closely
44 linked to energy dissipation where a higher density of local minima in PEL is more likely to trigger
45 cascade relaxations and thus may affect the primary damage production. Evaluation of potential energy
46 differences between initial minimum states and nearby saddle states on PEL with different local structure
47 (atomic arrangements) reveals that the susceptible atoms involved in deformation of metallic glasses can
48 be characterized by the correlations between atomic displacements and atomic stress changes.

49 The similarity of atomic-level chemical complexity and site-to-site inhomogeneity (lattice
50 distortion), yet on a relatively simple structure is the common characteristic in complex oxides, III-V
51 semiconductors, MBGs and CSAs. In CSAs, different from traditional alloys, the intrinsic lattice

1 distortions, the intricate electron-electron interactions [2,12], the complex energy landscapes, and local
2 stress fluctuations are shown to have profound effects on the mechanical properties [3-11], yet the
3 research effort to clarify links between these intrinsic variables and microstructural evolutions under non-
4 equilibrium radiation condition is just starting. Given the complexities of lattice distortion and atomic
5 stress fluctuation, the defects in CSAs are sitting in a wide range of distributions of local environments, in
6 contrast to the very explicit and narrow distributions in traditional alloys. It therefore makes the study of
7 microstructural evolutions in CSAs particularly challenging.

8 Effect of extreme chemical complexity on defect dynamics and radiation performance in
9 concentrated solid-solution alloys is an exciting field to explore. Given that relatively little is known of
10 extreme chemical effects on defect dynamics under thermal equilibrium condition, and even less known
11 about their impact in a high radiation environment that is far away from non-equilibrium condition, the
12 pioneering work on the *effects of chemical complexity on defect dynamics and radiation performance in*
13 *metals and alloys reviewed* in Section 3 and 4 is highly intriguing. There are many open questions,
14 including (1) how can we understand the intricate correlations of the atomic or electronic constituents in
15 CSAs? (2) how do the electronic and atomic subsystems respond to energy deposition separately and
16 collectively, and how can we control energy flow and mass transport during the correlated, non-adiabatic
17 electronic and atomic processes? (3) how do we understand, predict, and ultimately control the dynamics
18 of excited or non-equilibrium states, and to control matter away – especially very far away – from
19 equilibrium? and (4) how can we reveal underlying crucial knowledge for the development of
20 transformative materials with optimized functionality in extreme conditions.

21 The scientific challenges include (1) assessment of static structure in CSAs in terms of short- and
22 long-range elemental disorder, local stresses, lattice distortions, etc, and examination of how these
23 variable would influence the energy dissipation mechanisms (2) description of the complex energy
24 landscapes in CSAs, especially the temperature-dependent energy landscapes, as the changes of thermal
25 environments may lead to atoms rearrangements and also considerably modify energy dissipation as well
26 as the mass transport processes over a wide range of time and length scales; (3) exploration of early stages
27 of radiation damage beyond the current empirical description; and (4) prediction of the microstructural
28 evolution from the fundamental correlations between atomic level stress fluctuation and lattice distortion
29 (atomic displacement from ideal lattice site). The scientific understanding on diffusion in these alloys
30 will, for example, shed light on how to model diffusion in complex multi-component semiconductor
31 alloys that are increasingly being employed in new electronic devices. More importantly, the knowledge
32 may eventually reveal a unified description of chemical effects on irradiation performance in solids
33 (metals, alloys, metallic glasses, semiconductors, and insulators, etc).

34 6. Summary

35 Alloy development or innovation with much improved radiation resistance performance demands
36 taking advantage of property enhancements that go beyond linear extrapolation. A clear demonstration of
37 enhanced radiation resistance is reported by tailoring chemical disorder from pure Ni to binary and more
38 complex solid solutions. Recent research has revealed that changes in chemical complexity have
39 substantial influence on defect dynamic and damage accumulation in CSAs. Experimental and modeling
40 results in solid-solution alloys with various compositional complexities (binary, ternary, quaternary, and
41 quinary HEA solid solutions) have shown that defect production and subsequent recombination can be
42 modified. Systematically understanding of how material properties can be tailored by chemical
43 complexity and their influence on defect dynamics may pave the way for material by design at the level of
44 atoms and electrons, may inspire new design principles of radiation-tolerant structural alloys for advanced
45 energy systems and for new defect engineering paradigms benefiting broader science and technology.

46 While this review focuses on the intrinsic properties of concentrated solid-solution alloys,
47 advancement in nanotechnology should not be overlooked. Studies worldwide have shown that nano-
48 scale features can significantly affect defect dynamics and microstructural evolution [91,92]. Some
49 nanomaterials have shown to have high radiation tolerance including nanostructured crystalline materials,
50 such as Fe-based or Ni-based ODS alloys. Taking advantage of the existing knowledge from

1 nanotechnology, new knowledge from controlling chemical complexity together with the advances
2 achieved from incorporation of nano-scale features (e.g. low level of substitutional additions,
3 nanoparticles, grain boundaries, etc) in concentrated solid-solution alloys may lead to additional alloy
4 design criteria to meet various application requirements. While the work reviewed here is more closely
5 related to radiation effects, understanding the response of materials to energy deposition from unique
6 aspects of defect evolution is fundamentally important and can have broad interests that is not only
7 limited to advanced alloy design. The breakthrough in this open field will lead to science-based rational
8 accelerated material discovery and radical changes in the field of radiation effects that is not limited to
9 structural alloys.

10 Acknowledgements

11 YZ, SZ and WJW were supported as part of the Energy Dissipation to Defect Evolution (EDDE),
12 an Energy Frontier Research Center funded by the U.S. Department of Energy, Office of Science, Basic
13 Energy Sciences. KN, FG and FD were funded within the framework of the EUROfusion Consortium and
14 have received funding from the Euratom research and training program 2014-2018 under grant agreement
15 No 633053. The views and opinions expressed herein do not necessarily reflect those of the European
16 Commission. Ion beam work was partially performed at the University of Tennessee–Oak Ridge National
17 Laboratory Ion Beam Materials Laboratory (IBML) located at the campus of the University of Tennessee,
18 Knoxville. We thank H. Xue and K. Jin at the University of Tennessee for conducting the ion channeling
19 measurements. Part of the simulation used resources of the National Energy Research Scientific
20 Computing Center, supported by the Office of Science, US Department of Energy, under Contract No.
21 DEAC02-05CH11231.

22 References

1. Li Z, Pradeep KG, Deng Y, Raabe D, tasan CC. Metastable high-entropy dual-phase alloys overcome the strength-ductility trade-off. *Nature* 2016;534:227–230.
2. Zhang Y, Jin K, Xue H, Lu C, Olsen RJ, Beland LK, *et al.* Influence of Chemical Disorder on Energy Dissipation and Defect Evolution in Advanced Alloys. *J. Mater. Res.* 2016;31(16):2363–2375.
3. Gludovatz B, Hohenwarter A, Thurston KVS, Bei H, Wu Z, George EP, *et al.* Exceptional damage-tolerance of a medium-entropy alloy CrCoNi at cryogenic temperatures. *Nat. Commun.* 2016;7:10602.
4. Yeh JW, Chen SK, Lin SJ, Gan JY, Chin TS, Shun TT, *et al.* Nanostructured High-Entropy Alloys with Multiple Principal Elements: Novel Alloy Design Concepts and Outcomes. *Adv. Eng. Mater.* 2004,6:299–303.
5. Tsai MH, Yeh JW. High-Entropy Alloys: A Critical Review. *Mater. Res. Lett.* 2014; 2:107-123.
6. Zhang Y, Zuo TT, Tang Z, Gao MC, Dahmen KA, Liaw PK, *et al.* Microstructures and properties of high-entropy alloys, *Progress in Materials Science*, 2014;61:1–93.
7. Senkov ON, Wilks GB, Miracle DB, Chuang CP, Liaw PK. Refractory high-entropy alloys. *Intermetallics* 2010;18:1758-1765.
8. Senkov ON, Wilks GB, Scott JM, Miracle DB. Mechanical properties of Nb₂₅Mo₂₅Ta₂₅W₂₅ and V₂₀Nb₂₀Mo₂₀Ta₂₀W₂₀ refractory high entropy alloys. *Intermetallics* 2011;19:698-706.
9. Wu Z, Bei H, Pharr GM, George EP. Temperature dependence of the mechanical properties of equiatomic solid solution alloys with face-centered cubic crystal structures. *Acta Mater.* 2014;81: 428–441.
10. Gludovatz B, Hohenwarter A, Catoor D, Chang EH, George EP, Ritchie RO. A fracture-resistant high-entropy alloy for cryogenic applications. *Science* 2014;345:1153-1158.
11. Wei Y, Li Y, Zhu L, Liu Y, Lei X, Wang G, *et al.* Evading the strength–ductility trade-off dilemma in steel through gradient hierarchical nanotwins. *Nature Commun.* 2014;5:3580.

12. Zhang Y, Stocks GM, Jin K, Lu C, Bei H, Sales BC, *et al.* Influence of chemical disorder on energy dissipation and defect evolution in nickel and Ni-based concentrated solid-solution alloys. *Nat. Commun.* 2015;6:8736.
13. Granberg F, Nordlund K, Ullah MW, Jin K, Lu C, Bei H, *et al.* Mechanism of radiation damage reduction in equiatomic multicomponent single phase alloys. *Phys. Rev. Lett.* 2016;116:135504.
14. Lu C, Chen N, Niu L, Jin K, Yang T, Xiu P, *et al.* Enhancing radiation tolerance by controlling defect mobility and migration pathways in multicomponent single phase alloys, *Nature Commun.* 2016; Under review.
15. Troparevsky MC, Morris JR, Kent PRC, Lupini AR, Stocks GM. Criteria for Predicting the Formation of Single-Phase High-Entropy Alloys, *Phys. Rev. X* 2015;5:011041.
16. Jin K, Sales BC, Stocks GM, Samolyuk GD, Daene M, Weber WJ, *et al.* Tailoring the physical properties of Ni-based single-phase equiatomic alloys by modifying the chemical complexity. *Sci. Rep.* 2016;6:20159.
17. Jin K, Lu C, Wang LM, Qu J, Weber WJ, Zhang Y, *et al.* Effects of compositional complexity on the ion-irradiation induced swelling and hardening in Ni-containing equiatomic alloys. *Scr. Mater.*, 2016;119:65-70.
18. Wang LM, Dodd RA, Kulcinski GL. Gas effects on void formation in 14 MeV nickel ion irradiated pure nickel. *J. Nucl. Mater.* 1986;141-143:713-717.
19. Wang LM, Dodd RA, Kulcinski GL. Radiation damage and copper distribution in 14 MeV copper-implanted nickel - TEM and AEM analyses in cross-section, *Ultramicroscopy* 1989;29:284-290.
20. Wang LM, Zinkle SJ, Dodd RA, Kulcinski GL. Effects of preinjected helium in heavy-ion irradiated nickel and nickel-copper alloys. *Metallurgical Transactions A.* 1990;21:1847-1851.
21. Mitchell MA, Garner FA. Neutron-induced swelling of binary Ni-Al alloys, *J. Nucl. Mater.*, 1992;187:103-108.
22. Osetsky YN, Béland LK, Stoller RE. Specific features of defect and mass transport in concentrated fcc alloys, *Acta Mater.* 2016;115:364-371.
23. Lu C, Jin K, Béland LK, Zhang F, Yang T, Qiao L, *et al.* Direct observation of defect range and evolution in ion-irradiated single crystalline Ni and Ni binary alloys. *Sci. Rep.* 2016;6:19994.
24. King HW. Quantitative Size-Factors for Metallic Solid Solutions, *J Mater. Sci.* 1966;1:79-90.
25. Wakai E, Ezawa T, Imamura J, Takenaka T, Tanabe T, Oshima R. Effect of solute atoms on swelling in Ni alloys and pure Ni under He⁺ ion irradiation. *J. Nucl. Mater.* 2002;307-311:367-373.
26. Fukumoto K, Kimura A, Matsui H. Swelling behavior of V-Fe binary and V-Fe-Ti ternary alloys. *J. Nucl. Mater.* 1998;258-163:1431-1436.
27. Chernov II, Staltsov MS, Kalin BA, Mezina OS, Oo KZ, Chernov VM. Mechanisms of helium porosity formation in vanadium alloys as a function of the chemical composition. *Atomic Energy*, 2011;109:176-183.
28. Solonin MI. Radiation-Resistant Alloys of the Nickel-Chromium System, *Metal Science and Heat Treatment* 2005;47:328-332.
29. Votinov SN, Kolotushkin VP. Structural factor and effects of low-temperature radiation damage in structural materials, *Metal Science and Heat Treatment.* 2006;48:36-40.
30. Kolotushkin VP, Votinov SN. Structural factor and effects of low-temperature radiation damage in structural materials, *Metal Science and Heat Treatment.* 2006;48:452-458.
31. Little EA, Stow DA. Void-swelling in irons and ferritic steels: II. An experimental survey of materials irradiated in a fast reactor. *J. Nucl. Mater.* 1979;87:25-39.
32. Gelles DS. Microstructural examination of neutron-irradiated simple ferritic alloys. *J. Nucl. Mater.* 1982;515:108-109.
33. Gelles DS. Void swelling in binary FeCr alloys at 200 dpa. *J. Nucl. Mater.* 1995;225:163-174.
34. Kato Y, Kohyama A, Gelles DS. Swelling and dislocation evolution in simple ferritic alloys irradiated to high fluence in FFTF/MOTA. *J. Nucl. Mater.* 1995;225:154-162.

35. Porollo S I, Dvoriashin AM, Vorobyev AN, Konobeev YV. The microstructure and tensile properties of Fe-Cr alloys after neutron irradiation at 400°C to 5.5-7.1 dpa. *J. Nucl. Mater.* 1998;256:247–253.
36. Allen TR, Cole JI, Gan J, Was GS, Dropek R, Kenik EA. Swelling and radiation-induced segregation in austenitic alloys. *J. Nucl. Mater.* 2005;342:90–100.
37. Horton LL, Bentley J, Jesser WA. The depth distribution of displacement damage in α -iron under “triple beam” ion irradiation. *J. Nucl. Mater.* 1981;103-104:1085-1090.
38. Yao Z, Hernández-Mayoral M, Jenkins ML, Kirk MA. Heavy-ion irradiations of Fe and Fe-Cr model alloys Part 1: Damage evolution in thin-foils at lower doses, *Philosophical Magazine*, 2008;88:2851–2880.
39. Hernández-Mayoral M, Yao Z, Jenkins ML, Kirk MA. Heavy-ion irradiations of Fe and Fe-Cr model alloys Part 2: Damage evolution in thin-foils at higher doses. *Philosophical Magazine*, 2008;88:2881–2897.
40. Horiki M, Yoshiie T, Sato K, Xu Q. Point defect processes in neutron irradiated Ni, Fe-15Cr-16Ni and Ti-added modified SUS316SS, *Philosophical Magazine*. 2013;93:1701–1714.
41. Faulkner J, Stocks GM. Calculating properties with the coherent-potential approximation. *Phys. Rev. B* 1980;21:3222.
42. Zhao S, Stocks GM, Zhang Y, Defect energetics of concentrated solid-solution alloys from ab initio calculations: $\text{Ni}_{0.5}\text{Co}_{0.5}$, $\text{Ni}_{0.5}\text{Fe}_{0.5}$, $\text{Ni}_{0.8}\text{Fe}_{0.2}$ and $\text{Ni}_{0.8}\text{Cr}_{0.2}$. *Phys. Chem. Chem. Phys.* 2016,18:24043.
43. Zunger A, Wei S-H, Ferreira LG, Bernard JE. Special quasirandom structures. *Phys. Rev. Lett.* 1990;65:353.
44. Bonny G, Pasianot RC, Malerba L. Fe-Ni many-body potential for metallurgical applications. *Model. Simul. Mater. Sci. Eng.* 2009;17:25010.
45. Bonny G, Terentyev D, Pasianot RC, Poncé S, Bakaev A. Interatomic potential to study plasticity in stainless steels: the FeNiCr model alloy. *Model. Simul. Mater. Sci. Eng.* 2011;19:85008.
46. Bonny G, Castin N, Terentyev D. Interatomic potential for studying ageing under irradiation in stainless steels: the FeNiCr model alloy. *Model. Simul. Mater. Sci. Eng.* 2013;21:85004.
47. <http://www.ctcms.nist.gov/potentials/Ni.html>. No Title.
48. Caro A, Correa A, Tamm A, Samolyuk GD, Stocks GM. Adequacy of damped dynamics to represent the electron-phonon interaction in solids. *Phys. Rev. B.* 2015;92:144309.
49. Caro M, Béland LK, Samolyuk GD, Stoller RE, Caro A. Lattice thermal conductivity of multi-component alloys. *J. Alloy Compd.* 2015;648:408-413.
50. Tamm A, Aabloo A, Klintonberg M, Stocks GM, Caro A. Atomic-scale properties of Ni-based FCC ternary, and quaternary alloys. *Acta Mater.* 2015;99:307–312.
51. Samolyuk GD, Béland LK, Stocks GM, Stoller RE. Electron-phonon coupling in Ni-based binary alloys with application to displacement cascade modeling. *J. Phys.: Condens. Matter.*, 2016;28:17.
52. Aidhy DS, Lu C, Jin K, Bei H, Zhang Y, Wang L, *et al.* Point defect evolution in Ni, NiFe, and NiCr alloys from atomistic simulations and irradiation experiments, *Acta Mater.* 2015;99:69-76.
53. Ullah MW, Dilpuneet SA, Zhang Y, Weber WJ. Damage accumulation in ion-irradiated Ni-based concentrated solid-solution alloys. *Acta Mater.* 2016;109:17-22.
54. Aidhy DS, Lu C, Jin K, Bei H, Zhang Y, Wang L. Formation and growth of stacking fault tetrahedra in Ni via vacancy aggregation mechanism. *Scr. Mater.* 2016;114:137-141.
55. Egami T, Guo W, Rack PD, Nagase T. Irradiation resistance of multicomponent alloys. *Metall and Mat Trans A* 2014;45:180.
56. Nagase T, Rack PD, Noh JH, Egami T. In-situ TEM observation of structural changes in nanocrystalline CoCrCuFeNi multicomponent high-entropy alloy (HEA) under fast electron irradiation by high voltage electron microscopy (HVEM). *Intermetallics* 2015;59:32.
57. Egami T, Ojha M, Khorgolkhuu O, Nicholson DM, Stocks GM. Local electronic effects and irradiation resistance in high-entropy alloys. *JOM* 2015;67:2345.

58. Abhaya S, Rajaraman R, Kalavathi S, David C. Panigrahi BK, Amarendra G. Effect of dose and post irradiation annealing in Ni implanted high entropy alloy FeCrCoNi using slow positron beam. *J. Alloys & Compounds* 2016;669:117-122.
59. Olsen RJ, Jin K, Lu C, Béland LK, Wang LM, Bei H, et al. Investigation of defect clusters in ion-irradiated Ni and NiCo using diffuse X-ray scattering and electron microscopy. *J. Nucl. Mater.* 2016;469:153–161.
60. Chang KJ, Cohen Marvin L, Rhombohedral phase stability of the group-VA elements. *Phys. Rev. B.* 1986;33(10):7371–7373.
61. Béland LK, Lu C, Osetsky YN, Samolyuk GD, Caro A, Wang L, at al. Features of primary damage by high energy displacement cascades in concentrated Ni-based alloys *J. Appl. Phys.* 2016;119:085901.
62. Béland LK, Osetsky YN, Stoller RE. Atomistic material behavior at extreme pressures. *npj Computational Materials*, 2016;2:16007.
63. Stoller RE, Tamm A, Béland LK, Samolyuk GD, Stocks GM, Caro A, et al. The Impact of Short-range Forces on Defect Production from High-energy Collisions. *J. Chem. Theory Comput.*, 2016;12:2871–9.
64. Sand AE, Nordlund K, Dudarev SL. Radiation damage production in massive cascades initiated by fusion neutrons in tungsten. *J. Nucl. Mater.* 2014;455:211.
65. Sand AE, Dequeker J, Becquart CS, Domain C, Nordlund K. Non-equilibrium properties of interatomic potentials in cascade simulations in tungsten *J. Nucl. Mater.* 2016; 470, 119–127
66. Zhou XW, Johnson RA, Wadley HNG. Misfit-energy-increasing dislocations in vapor-deposited CoFe/NiFe multilayers. *Phys. Rev. B*, 2004;69:144113.
67. Zarkadoula E, Samolyuk G, Xue H, Bei H, Weber WJ. Effects of two-temperature model on cascade evolution in Ni and NiFe. *Scr. Mater.*, 2016; 124: 6–10.
68. Béland LK, Brommer P, El-Mellouhi F, Joly J-F, and Mousseau N. Kinetic Activation Relaxation Technique. *Physical Review B*, 2011;84:4.
69. N. Mousseau *et al.* Following atomistic kinetics on experimental timescales with the kinetic Activation-Relaxation Technique. *Computational Materials Science*, 2015;100:111–123.
70. Xu H, Osetsky YN, Stoller RE. Simulating complex atomistic processes: On-the-fly kinetic monte carlo scheme with selective active volumes/ *Physical Review B* 2011;84:132103.
71. Sickafus KE, Minervini L, Grimes RW, Valdez JA, Ishimaru M, Li F, et al., Radiation tolerance of complex oxides. *Science* 2000;289:748-51.
72. Lian J, Wang LM, Sun K, Ewing RC. In situ TEM of radiation effects in complex ceramics. *Microscopy Research and Technique* 2009;72:165–181.
73. Trachenko K, Understanding resistance to amorphization by radiation damage *J. Phys.: Condens. Matter* 2004;16:R1491–R1515.
74. Devanathan R, Weber WJ, Gale JD. Radiation tolerance of ceramics—insights from atomistic simulation of damage accumulation in pyrochlores. *Energy Environ Sci* 2010;3:1551–9.
75. Lang M, Toulemonde M, Zhang JM, Zhang FX, Tracy CL, Lian J, at al. *Nucl. Instrum. Methods Phys. Res. B* 2014;336:102–115.
76. Lian J, Chen J, Wang LM, Ewing RC, Farmer JM, Boatner LA, at al. *Phys Rev B* 2003;68:134107.
77. Lian J, Helean KB, Kennedy BJ, Wang LM, Navrotsky A, Ewing RC. *J Phys Chem B* 2006;110:2343–2350.
78. R. C. Ewing, W. J. Weber, J. Lian, *J. Appl. Phys.* 95 (2004) 5049.
79. Wang SX, Wang LM, Ewing RC, Was GS, Lumpkin GR. *Nucl Instrum Methods Phys Res B* 1999;148:704–709.
80. Wendler E, Wendler L. Empirical modeling of the cross section of damage formation in ion implanted III-V semiconductors. *Appl. Phys. Lett.*, 2012;100:192108.

81. Turkot BA, Lagow BW, Robertson IM, Forbes DV, Coleman JJ, Rehn LE, Baldo PM. Depth dependence of ion implantation damage in $\text{Al}_x\text{Ga}_{1-x}\text{As}/\text{GaAs}$ heterostructures. *J. Appl. Phys.*, 1996;80(8):4366.
82. Karsten K. and Ehrhart P. Frenkel pairs in low-temperature electron-irradiated InP: X-ray diffraction. *Phys. Rev. B*, 1995;51(16):10508.
83. Sayed M, Jefferson JH, Walker AB, Gullis AG. Computer simulation of atomic displacements in Si, GaAs and AlAs. *Nucl. Instr. Meth. Phys. Res. B*, 1995;102:232.
84. Björkas C, Nordlund K, Arstila K, Keinonen J, Dhaka VDS, Pessa M. Light and heavy ion effects on damage clustering in GaAs quantum wells. *Nucl. Instr. Meth. Phys. Res. B*, 2007;257:324.
85. Partyka P, Averback RS, Forbes DV, Coleman JJ, and Ehrhart P. X-ray diffraction and channeling-rutherford backscattering spectrometry studies of ion implantation damage in $\text{Al}_x\text{Ga}_{1-x}\text{As}$. *J. Appl. Phys.*, 1998;83(3):1265.
86. Vitek V, Egami T. Atomic Level Stresses in Solids and Liquids. *Physica status solidi (b)* 1987;144:145–156.
87. Schuh CA, Lund AC. Atomistic basis for the plastic yield criterion of metallic glass, *Nat. Mater.* 2003;2:449.
88. Egami T. Understanding the properties and structure of metallic glasses at the atomic level. *Bulk Metallic Glasses / Research Summary. JOM* 2010; 62:70-75.
89. Fan Y, Iwashita T, Egami T. How thermally activated deformation starts in metallic glass *Nature Commun.* 2014;5:5083.
90. Fan Y, Iwashita T, Egami T. Crossover from localized to cascade relaxations in metallic glasses. *Phys. Rev. Lett.* 2015;115:045501.
91. Krasheninnikov AV, Nordlund K, Ion and electron irradiation-induced effects in nanostructured materials. *J. Appl. Phys. (Applied Physics Reviews)* 2010;107:071301.
92. Nordlund K, and Djurabekova F, Multiscale modelling of irradiation in nanostructures. *J. Comput. Electr.* 2014;13:122.